login

- Home
- News
- Speaker/Poster information
- Preliminary Programme
- Preliminary Programme on abstract number
- Programme Information
- Conference Topics
- Awards
- Research Market/Beer & Wine Party
- Bedrijvenmarkt
- Invited Speakers
- Important Dates
- Registration and Venue
- Authors Instructions
- Organizing Board
- Contact

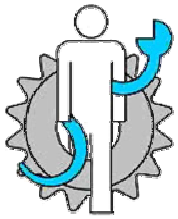

15:00 **Foyer: Poster Session Even numbers**

IN VITRO DEGRADATION BEHAVIOUR AND SURFACE BIOACTIVITY OF MAGNESIUM-MATRIX COMPOSITES FOR ORTHOPAEDIC APPLICATIONS

Zhiguang Huan, Sander Leeflang, Jie Zhou, Jurek Duszczyk

Abstract: Magnesium has been proven to be biosafe and biocompatible. Appropriate alloying and microstructure control can improve the degradation rate of magnesium. A number of alloys such as those containing zinc and zirconium have shown a great potential as biodegradable materials for orthopaedic applications. A modern orthopaedic implant material is desired to be bioactive so as to speed up the early tissue response. In the present research, bioactive particles (bioglass, 45S5) were introduced into a biocompatible magnesium alloy (ZK30) to form metal matrix composites (MMCs) in order to enhance the bioactivity of the matrix alloy. The MMCs were fabricated by using a semi-solid high-pressure casting method (SSC) and a powder metallurgy (P/M) method. Biocomposites with the same volume fractions of bioglass (BG) particles were compared. Microstructural observation indicated homogeneous dispersion of BG particles in the composites produced through both of the routes. SEM and EDX analysis showed the retention of the morphological characteristics and composition of BG particles in the composites. The as-cast composites showed a micro-porous structure, whereas the P/M composites had a much more densified structure. As compared with the ZK30 matrix alloy, the as-cast composites exhibited significantly accelerated degradation rates due to porosity, while the P/M composites possessed degradation rates similar to the degradation rate of the matrix alloy. On the surface of all the composites studied, accelerated deposition of Ca and P ions was confirmed after immersion tests in the cell culture medium for seven days, indicating an improved surface bioactivity of these composites. The results clearly showed that the P/M fabrication method is advantageous over the casting method and offers the possibility of yielding composite materials with enhanced early-stage bioactivity for implants without sacrifice in degradation characteristics.

LONG-TERM IN VITRO BIODEGRADATION BEHAVIOUR AND MECHANICAL PROPERTIES OF MG-LI-BASED ALLOYS FOR BIOMEDICAL APPLICATIONS

Sander Leeflang, Joanna Dzwonczyk, Jie Zhou, Jurek Duszczyk

Abstract: In recent years, magnesium alloys have become increasingly interesting materials for orthopaedic and cardiovascular applications, because of their biodegradability, good biocompatibility, low Young's modulus and moderate strength. The vast majority of the in vitro and vivo studies conducted so far have been on commercial grades of magnesium alloys, originally designed for general engineering applications. Inconsistent results have been obtained from in vivo tests; the formation of gas pockets around the implant and fracture of the implant have been observed. It is obvious that new alloys with enhanced ductility, moderate degradation rate and hydrogen evolution rate must be developed. It is well known that when alloyed with 5.5 to 11 wt. % lithium, magnesium changes its lattice structure from a hexagonal close packed (HCP) one to a dulpex structure with a combination of a body centred cubic (BCC) one and HCP, thereby offering a balance between strength and ductility around the normal body temperature of 37 0C. In order to compensate for the loss in strength due to lithium addition, small amounts of aluminium and rare-earth elements may be added. These alloying elements have shown positive effects on the short-term corrosion resistance. However, the degradation rates, associated hydrogen evolution rates of these alloys in a chloride-containing solution such as the human body fluid over a period of time as clinically required, as well as their mechanical properties, are unknown. The present research aimed at determining the long-term in vitro biodegradation rates, hydrogen evolution rates and mechanical properties of three Mg-Li-Al-(RE) alloys with different concentrations of aluminium and rare-earth elements, i.e. Mg-9Li-1Al (LA91), Mg-9Li-1Al-2RE (LAE912) and Mg-9Li-2Al-2RE (LA922). Comparisons were made with a WE-type alloy. Immersion tests in Hank's solution over a period of 600 days were carried out. The results showed higher degradation rates of LAE912 and LAE922, but a significantly lower degradation rate of LA91, in comparison with that of the WE-type alloy. It is thus clear that an addition of rare-earth elements accelerates the degradation of the Mg-9Li alloy, while an increase in aluminium concentration slows down its degradation. Hydrogen evolution of LA91 associated with degradation was much lower than that of any of the other alloys investigated. Moreover, the extruded LA91 alloy possessed a highly desired elongation to facture value of 33%, which nearly doubled the value of the WE-type alloy. An addition of rare-earth elements to the LA91 alloy led to a further increase of elongation, but a sacrifice in yield strength. In short, with respect to the degradation rate, hydrogen evolution rate and mechanical properties, LA91 appeared to be the alloy of the greatest interest for biomedical applications and it is worth further in vitro and in vivo investigations.

MOTION CORRECTION AND SPECTRAL UNMIXING IN TIME-RESOLVED FLUORESCENCE IMAGING

Martijn van de Giessen, Jouke Dijkstra, Clemens Lowik, Hans Tanke, Cock van de Velde, Alexander Vahrmeijer, Hans Reiber, Boudewijn Lelieveldt

Abstract: The goal of this project is to develop a multi-spectral camera system for tumor and metastases detection during oncological surgery. The use of temporal image information requires estimates of spatial correspondence between frames, i.e. registration in the case of motion. To this end a motion correction algorithm has been developed that can handle local intensity changes between frames. To separate fluorescent tumor marker signal from background noise and responses from different fluorescent markers, several spectral unmixing algorithms have been investigated. Motion correction Materials and methods: Awaiting clinical data, sequences of fluorescence data with biological cell markers were used, where different regions were bleached with different attenuations. By estimating a simple model of the bleaching process, motion artifacts show up as spurious intensity changes, which can be minimized by assuming a small, but unspecified number of different attenuation magnitudes. Results: The proposed motion reduction algorithm minimized motion artifacts and thereby revealed previously indiscernible details. The algorithm can cope with high noise levels. Spectral unmixing Materials and methods: Using images of animal models, injected with multiple probes, several linear unmixing algorithms were investigated that assumed a varying degrees of prior knowledge about the fluorescence spectra. Results: Unconstrained spectral unmixing algorithms allowed (incorrectly) for negative photon counts. Constrained spectral unmixing correctly yielded semi-positive photon counts. Blind source separation using nonnegative matrix factorization (NMF) gave similar results as quadratic programming, but without prior knowledge about the spectra. Quadratic programming however, was much faster, and is promising for real-time implementation. Conclusions By estimating a simple model of the intensity variations only weak assumptions are needed to correct for motion between subsequent frames. Constraints are necessary to obtain physically feasible spectra for linear spectral unmixing. NMF is capable of blind source separation, but not in real-time. By including prior knowledge we hope to adapt the NMF algorithm to allow real-time application. This research was supported by the Center for Translational Molecular Medicine (MUSiS)

EARLY VERIFICATION AND VALIDATION OF USER REQUIREMENTS IN TELE-REHABILITATION

Rianne Huis in 't Veld, Miriam Vollenbroek-Hutten, Hermie Hermens

Abstract: Tele-rehabilitation has the great potential to provide cost-effective at-home services for disabled persons. Despite its great potential, professionals and patients often face a tele-rehabilitation system which does not completely meet their needs. As a solution, sociotechnical approaches emphasize the continuous involvement of users, i.e. patients and clinicians, in the design trajectory. However, due to the fact that tele-rehabilitation services have hardly been deployed, (part of the) users have no prior experience of the potentialities of information technology in rehabilitation care; they neither know the requirements, nor they can articulate them [1]. Miscommunication and misinterpretation between users and the design team is likely to occur. To minimize this risk, we advocate the early verification and validation of the requirements obtained. We developed a methodology that aims at an early verification and validation of the requirements. The methodology makes a distinction between service and systems requirements. Service requirements define 'what should be delivered how' in order to create value for users. In turn, the service requirements provide input for the systems requirements. For service validation, perspective based scenario reading and visualization is applied [2]. For system validation we used checklist-based reading techniques; a technique which includes questions which guide the validation. This paper demonstrates the practical application and experiences with this methodology in the development of an exercise-based tele-rehabilitation platform for patients with pulmonary and musculoskeletal disorders. Eight professionals and eight patients were assigned a specific perspective (patient or professional) to detect incompleteness, inconsistencies and faults in the scenario describing the service delivery. In addition, they completed the questions related to the list of system requirements after a demonstration and hands-on experience with the (prototype version) of the system. The early validation of service and systems requirements are hypothesized to increase the comprehension and understanding of the users, thereby enabling the generation of important feedback for services and systems under development. The better we are able to validate requirements the better the chances of successfully implementing and deploying them.

MORPHOLOGY-BASED BONE LOADING ESTIMATION

Patrik Christen, Bert van Rietbergen, Floor Lambers, Ralph Müller, Keita Ito

Abstract: Background: It is generally accepted that bone density and microarchitecture are the result of a load-adaptive bone

remodeling process in which bone strives for uniform tissue loading ('Wolff's law') [1]. This implies that, in turn, it would be possible to calculate an unknown loading history by finding the set of forces that produces uniform tissue loading. Such a procedure for the determination of bone loading history on the basis of bone density and architecture would be of great importance to derive estimates of bone loading conditions for bone remodeling studies. Objective: The aim of this study was to exploit and test this concept for test grid models and for a set of mice bones with known loading history. Methods: Micro-finite element models of artificially created grid structures and mice tail vertebrae were generated. Vertebra models were based on in vivo micro-CT scans made from two groups, one that received daily in vivo loading at 8 N and one with no additional loading which served as control group [2]. Forces were sequentially applied and scaling factors were calculated for each force to determine the most uniform tissue strain-energy density (SED) when all scaled forces are applied simultaneously. Results: Forces in the direction of the grid struts were predicted as the dominant loading directions and little remaining variation in tissue SED was found. Compression was predicted as the main load case for the mice vertebrae, with an average of 8.2 N for the loaded group and 5.5 N for the control group. In both groups, considerable inhomogeneity in tissue SED remained. Conclusion: The approach introduced here, successfully predicted the expected external forces for both grid models and was able to predict the difference in loading history to which the mice vertebrae were adapted. Therefore, we conclude that the results obtained here are encouraging and that bone loading estimations based on its morphology could be useful for bone remodeling studies or other investigations where measurements are difficult or impossible such as for bone in vivo or fossil bones.

SHAPE ESTIMATION OF PERCUTANEOUS INSTRUMENTS WITH FIBER BRAGG GRATINGS
Kirsten Henken, John van den Dobbelsteen, Jenny Dankelman
Abstract: Kirsten R. Henken*, John J. van den Dobbelsteen and Jenny Dankelman *Delft University of Technology, Mekelweg 4, 2628 CD Delft The Netherlands e-mail: K.R.Henken@tudelft.nl ABSTRACT Currently no system exists that is able to access all regions of the body with minimal damage to healthy tissue. The most advanced systems for percutaneous interventions available today, use rigid needles that cannot circumvent critical organs, or they use passive flexible instruments that are difficult to navigate from the outside of the patients body. The aim of the project PITON (percutaneous instruments tele-operated needles) is to develop steerable MRI compatible robotic instruments with precise force sensing for accurate tissue characterization and accurate curvature estimation for dexterous navigation in percutaneous interventions. To estimate the curvature of such a steerable instrument, strain is measured in the instrument with fibers equipped with FBG's (Fiber Bragg Gratings). This principle has already been investigated by Park et al. [1, 2]. Therefore, three fibers equipped with several FBG's are glued together into a fiber triplet. Based on the relative strain measured in the triplet and a geometric model, curvature of the triplet is estimated. Measurements will be performed with the triplet in a silicon tube to identify the accuracy, precision, and reproducibility of curvature estimation. Then the triplet is assembled in a 2 mm diameter instrument with two steering segments to investigate the performance of the triplet in a real environment. The steering of the instrument is based on the cable-ring mechanism previously developed by TU Delft. In the experiments, several predefined radii or displacements are applied to the tube or instrument, after which strain is measured and the curvature of the tube or instrument is estimated. The results are compared to the curvature estimated based on photographs. Results and conclusions will be presented on the conference. REFERENCES [1] Y.L. Park, S. Elayaperumal, B.L. Daniel, E. Kaye, K.B. Pauly, R.J. Black, and M.R. Cutkosky, "MRI-compatible Haptics: Feasibility of using optical fiber Bragg grating strain-sensors to detect deflection of needles in an MRI environment," Int. Soc. for Magnetic Resonance in Med.(ISMRM), (2008). [2] Y.L. Park, S. Elayaperumal, S. Ryu, B. Daniel, R.J. Black, B. Moslehi, and M. Cutkosky, "MRI-compatible Haptics: Strain sensing for real-time estimation of three dimensional needle deflection in MRI environments." Int. Soc. for Magnetic Resonance in Med.(ISMRM), (2009).

OBSERVING DYNAMIC CHANGES IN SKIN CHROMOPHORE CONCENTRATIONS AND SKIN TEMPERATURES USING HYPER-SPECTRAL AND THERMAL IMAGING TECHNIQUES
John Klaessens, Herke Jan Noordmans, Rowland de Roode, Ruud Verdaasdonk
Abstract: Assessing pathologic or physiologic conditions of tissue can be a challenging task, normally this is determined by visual inspection or with point measurements over time. With the advent of multi-spectral(1) and thermal imaging (2)techniques it has become possible to study physiologic changes in a more quantitative way. This because recently the signal-to-noise ratio of the equipment has considerably improved which makes it now possible to image low light intensities over a longer time period. Static applications are the extent of skin cancer, of early inflammation, or of diabetic feet injuries, while dynamic applications are that of imaging of local changes in oxygenation, blood perfusion, or temperature to study the process of wound healing or skin progression. As an example we measured the changes in oxygenation on the brain cortex caused by a repeating epileptic seizure occurring every 6 minutes showing large correspondence with intra-cortical EEG recordings (figure 1). A thermal example is shown in figure 2 where skin temperature images were acquired with an IR thermal camera of patients undergoing a local anesthetic block. Anesthetics were performed by administering Ropivacaine around the plexus brachialis. This causes nerve blocks towards the arm and hand resulting in dilatation of the blood vessels which induce an increase of blood flow and, consequently, an increase of the skin temperature and skin oxygenation in the lower arm and hand. Both multi-spectral imaging techniques and the thermal imaging technique show promising results for detecting dynamic changes in the hemoglobin concentrations and temperature distributions. References (1) Wieringa, F. P.; Mastik, F.; van der Steen, A. F. Contactless Multiple Wavelength Photoplethysmographic Imaging: a First Step Toward "SpO2 Camera" Technology. Ann. Biomed. Eng 2005, 33, 1034-1041. (2) Galvin, E. M.; Niehof, S.; Medina, H. J.; Zijlstra, F. J.; van, B. J.; Klein, J.; Verbrugge, S. J. Thermographic Temperature Measurement Compared With Pinprick and Cold Sensation in Predicting the Effectiveness of Regional Blocks. Anesth. Analg. 2006, 102, 598-604.

VALIDATION OF DCE-MRI ARAMETRIC MAPS: DEVELOPING A TOOL USING 3D-HISTOLOGY
Karin Bol, Joost Haeck, Lejla Alic, Monique Bernsen, Marion de Jong, Wiro Niessen, Jifke Veenland
Abstract: The purpose of this study is to develop a validation tool for DCE-MRI parametric maps of tumour tissue, based on exact co-registration of MRI with 3D-histology. In literature, many different DCE-analysis methods are used to characterize tumour tissue. To validate these methods histology is the gold standard and exact co-localization between histology and MR images is therefore a prerequisite. This co-localization is complicated by deformation and shrinking of the tissue during histological processing. To meet this problem, a pancreatic tumour (CA20948) was grown in a rat model and imaged with MRI using DCE-MRI, T1- and T2*-weighted sequences. After in-vivo MR imaging, the tumor was dissected, frozen, and cut into thin slices. These slices were stained with haematoxylin and eosin, digitized and stacked in a 3D volume. The 3D-histology stacks were registered to DCE-MRI images using non-rigid B-splines with a mutual information metric. Semi-quantitative and quantitative parameters (using a two-compartment model) were computed from the DCE data. For the evaluation, regions of interest (ROI's) consisting of vital and non-vital tumour tissue were drawn in histology and transformed to DCE-parametric maps. Results show that in quantitative DCE-MRI parametric maps, the average values in vital and non-vital ROI's were significantly different for the standard Tofts Model. For the semi-quantitative parameters, a significant difference between vital and non-vital tissue was observed for the wash-in, wash-out, maximum enhancement and Area under the Curve (AUC). Whereas the Tofts Model and the wash-in parameters can discriminate between vital and non-vital tissue, the wash-out, maximum enhancement and the AUC showed large overlap between vital and non-vital tissue. Therefore we conclude that only the pharmacokinetic DCE-parameters, and the heuristic parameter wash-in, can discriminate between vital and non-vital tumour regions. However, non-rigid registration is necessary for exact co-localization of DCE-MRI data with histology. In future, this method will be expanded to evaluate several quantitative DCE-MRI analysis methods.

SKIN CHARACTERISTICS AND PSYCHOPHYSICAL ASPECTS OF VIBROTACTILE STIMULATION FOR FEEDBACK IN FOREARM PROSTHESES
Heidi Witteveen, Hans Rietman, Peter Veltink
Abstract: Vibrotactile stimulation seems to be a good solution to provide feedback about force and level of hand opening in a forearm prosthesis in a comfortable and non-obtrusive way. However, the interpretation of the stimulus is influenced both by the mechanical characteristics of the skin and the mechanoreceptor properties. In this study, skin characteristics and psychophysical aspects are evaluated during vibrotactile stimulation in a parallel direction to the skin at 3 different locations on the arms of 10 healthy subjects. Vibrotactile stimulation was performed by a small pager motor fixed to the skin by double sided tape. Mechanical characteristics mass, damping and stiffness are calculated from the best fit of the corresponding transfer function on the measurement data. Stimulus interpretation by the user was investigated by evaluation of the just noticeable differences (JNDs) and the psychophysical method of magnitude estimation. It was shown that the mechanical characteristics at the outer side of the elbow were different from the other locations. However, no significant differences between stimulation locations were found for the psychophysical properties, which could indicate the compensation of the differences in skin mechanics by the mechanoreceptor properties. The derived just noticeable differences were much smaller the minimal distance between stimulation frequencies that could be distinguished after magnitude estimation, which proposes the use of stimulus changes instead of absolute intensities to provide feedback in future applications.

EVALUATION AND CORRECTION OF LUMEN CONTRAST-ENHANCEMENT INFLUENCE TO NON-CALCIFIED CORONARY ATHEROSCLEROTIC PLAQUES VISUALIZATION ON CT
Wisnumurti Kristanto, Peter van Ooijen, Matthijs Oudkerk
Abstract: Background: Coronary artery disease is a thickening of the wall of the artery as plaques build up in it. Certain type of plaque can suddenly rupture and block the coronary artery. With Computed tomography (CT) non-calcified plaque can be characterized by virtue of each plaque's specific Hounsfield Unit (HU) value.1 However, non-calcified plaques HU values can be influenced by the HU values of the contrast agents which used to visually enhance the lumen.2 This study aims to evaluate and develop an algorithm to correct for this lumen contrast-enhancement influence in order to facilitate HU-based non-calcified plaque characterization. Material and Methods: Three coronary vessel phantoms with circular lumen of diameter 1, 2, and 4mm, a normal

wall (3mm thick and 35HU), and a plaque-infested wall (2mm thick and -10HU) were scanned simultaneously with dual-source CT (120kV, 300mAs/rot, 64x0.6mm). The scans were repeated as the lumen was alternately filled with water and with 4 contrast solutions (100, 200, 300, and 400HU). The images were reconstructed at 0.6/0.4mm thickness/increment using 200mm field-of-view (x-y pixel size: 0.4mm). The walls' (normal and plaque-infested) and lumen's HU values were measured inside regions of interest matching the designed morphology. Whenever possible, a semi-automatic vessel segmentation was performed.3 Pixel-by-pixel comparisons between contrast-enhanced and non-contrast-enhanced images (reference for uninfluenced wall) were performed to extract the lumen contrast-enhancement influence. Results: The wall and lumen HU values were positively linearly correlated ($r2 = 0.96$), with approximately the same gradients for both wall types. The patterns of the extracted lumen contrast-enhancement influence were following exponential lines ($y=Ae-\lambda x+C$) from the lumen border, with the A's and the C's linearly correlated to the mean lumen HU values and the λ's relatively constant. Outside a 2-pixel radius, the median difference of mean wall values to the reference was 2HU. Inside a 2-pixel radius, the median difference of mean wall values to the reference was 44HU. Applying the exponential lines to correct for the lumen influence on this part of the wall managed to reduce the median difference of the inside 2-pixel radius to the reference to 1HU. Conclusion: Non-calcified plaques values were influenced by lumen contrast-enhancement exponentially until 2-pixels radius from lumen border. Application of the correction algorithm managed to correct the plaque HU value to a median difference of 1HU. References [1] Schroeder S, et al., J Comput Assist Tomogr,Vol.28, pp.449, (2004). [2] Cademartiri F, et al., Eur Radiol,Vol.15, pp.1426-1431, (2005). [3] Kristanto W, et al., Int J Cardiovasc Imaging,Vol.26, pp.77-87, (2010).

MOTOR CORTEX STIMULATION: THE SIGNIFICANCE OF MODELLING AXON COLLATERALS
Daphne Zwartjes, Tjitske Heida, Peter Veltink
Abstract: Motor cortex stimulation (MCS) is an increasingly applied treatment for pain and movement disorders, such as Parkinson's disease. In order to gain understanding of the underlying mechanisms of MCS, models have been developed (Manola et al. 2007). These models demonstrated that cathodal stimulation preferentially excites horizontally oriented fibers, whereas anodal stimulation preferentially excites vertically oriented fibers. The vertical fibers are mainly pyramidal tract neurons and the horizontal fibers may represent axon collaterals of pyramidal tract neurons, bifurcations of thalamo-cortical or cortico-cortical neurons and inhibitory neurons. It has been suggested that MCS activates both the excitatory pyramidal tract neurons and the inhibitory neurons (Arle and Shils 2008; Hanajima et al. 2002). It is thought that the balance between the activation of both neuronal populations determines the clinical effect on the treatment of pain and movement disorders. Arle and Shils (2008) suggest that clinically effective MCS mainly activates the inhibitory population, but this is not proven. Modeling the activation of both populations using different stimulation protocols will provide more insight into this. Considering the models of pyramidal tract neurons, previous models represented this population as one vertical fiber, without collaterals (Manola et al. 2007). We developed a volume conduction model of the motor cortex stimulation and merged this with an axon model of the pyramidal tract neuron. A model incorporating these collaterals was compared to a model without collaterals. In this research, we show that adding collaterals to the pyramidal tract axon models highly influences model outcomes. Especially during cathodal stimulation, when the threshold for activation is greatly reduced when the collaterals are included in the model. Implementing these collaterals in the pyramidal neuron model is essential for understanding the mechanisms involved in MCS for the treatment of pain and movement disorders.

CELL-MATRIX INTERACTIONS IN ENGINEERED CARDIOVASCULAR TISSUE
Nicky de Jonge, Carlijn Bouten, Frank Baaijens
Abstract: Collagen is the main load bearing component of the extracellular matrix of cardiovascular tissues and is therefore a key factor when creating functional tissue engineered (TE) cardiovascular constructs. To control the mechanical behavior of these constructs, we aim to influence the tissue's collagen architecture through mechanical conditioning [1] or optimizing the micromechanical environment of the cell with scaffolds. Cells respond to these cues by actively remodeling the collagen matrix, but the underlying mechanisms are not fully understood. We want to dissect the influence of collagen resynthesis and reorganization through cell-matrix adhesions under various conditions of mechanical conditioning. For this purpose a high-throughput experimental model system of myofibroblasts in a matrix environment will be developed that allows for qualitative and real-time analysis of collagen architecture on a micrometer-scale. The outcomes of the project will be used for optimizing conditioning protocols and scaffolds for cardiovascular TE. As a first model, we aim to study remodeling without scaffold by using a myofibroblasts-seeded, constrained fibrin gel. This model will be further developed to a micro-scale system to quantify the effects of mechanical conditioning (collagen architecture, tissue mechanical properties) in real-time and a high-throughput fashion.

SUBACROMIAL IMPINGEMENT SYNDROME: THE IDENTIFICATION OF ETIOLOGIC MECHANISMS (SISTIM)
Pieter Bas de Witte, Jochem Nagels, Rob Nelissen, Jurriaan de Groot
Abstract: Introduction: The subacromial impingement syndrome (SIS), which can be characterized by pain with arm abduction, is the most prevalent disorder of the shoulder in primary health care. Its etiology is not clearly understood. Conservative treatment focuses at subacromial tissue inflammation processes or pathologic scapulohumeral motion patterns, while surgical treatment is primarily focused at spatial relief through resection of the anterior part of the acromion.1 However, reported results vary and are often mediocre (successful in 48- 90%).2 Our hypothesis is that SIS ("a lack of subacromial space") can be caused by 1) intrinsic muscle or tendon disorders, such as degenerative tendinopathy of the rotator cuff, resulting in a subacromial inflammatory reaction (fibrosis and edema) or proximal humerus translation, or 2) extrinsic spatial subacromial narrowing related to the shape of the scapular acromion and the humeral head. We believe patients should be treated according to their prominent etiological mechanism(s). Rotator cuff tears are an exponent example for intrinsic tendon disorders. In patients with this diagnosis, we recently identified a conflict between glenohumeral stability, arm mobility and (EMG) muscle activation patterns.3,4 We will apply the methods developed in these studies to study and identify etiological mechanisms in SIS. Objective: To discriminate etiological mechanisms in patients with SIS, to improve diagnostic and therapeutic strategies of SIS and to design concept diagnostics and treatment flow charts for each etiologic subgroup. Main study parameters: 1. Clinical phenotype (Clinical scores); 2. Bony shape parameters (segmented MRI); 3. Kinematic subacromial narrowing (3D motion tracking + bony shape (MRI)); 4. Subacromial tissue evaluation; i.e. inflammatory reactions, partial tendon tears (MRI); 5. Translation of the humerus (2D acromiohumeral distance on AP-radiographs during EMG-recorded isometric ab- and adduction force-tasks)6; 6. Dynamic muscle activation patterns of shoulder and rotator cuff muscles (EMG)3 References: [1] Neer, C. S. J. Bone Joint Surg. Am. 54:41-50, 1972 [2] Henkus, H. E. et al. J. Bone Joint Surg. Br. 91:504-510, 2009 [3] Steenbrink et al, J.Biomech. 42:1740–1745, 2009 [4] Steenbrink et al, J.Biomech. 43: 2049–2054, 2010 [5] Krekel et al. (2010) DOI: 10.1111/j.1467-8659.2009.01681.x [6] de Witte et al (2010) International Shoulder Group conference presentation

LISTENING TO BRAIN ACTIVITY: PHOTOACOUSTIC IMAGING AS FUNCTIONAL BRAIN IMAGING TECHNIQUE
Abraham van Duijn, Jithin Jose, Roy Kolkman, Srirang Manohar, Richard van Wezel
Abstract: Photoacoustic imaging (PAI) is a relatively new, non-invasive imaging modality in biomedicine, which measures laser induced ultrasound from blood and other absorbers in tissue. Short (nanosecond), non-ionizing, near-infrared laser pulses are directed to locally heat tissue (in the order of millikelvins), leading to thermo-elastic expansion, which causes the emission of acoustic pressure waves at ultrasound frequencies. These waves can be detected using broadband ultrasonic transducers and with the use of certain algorithms absorption contrast images can be reconstructed. Optical absorption in tissues can be endogenous, at these wavelengths mainly due to hemoglobin and melanin, or exogenous, using contrast agents. Since ultrasound waves undergo considerably less scattering in tissue compared with light, high resolution can be attained. In this study we explore the possibilities of applying photoacoustic imaging for functional brain imaging in small animals. The current gold standard in neuroimaging (fMRI) measures the signal changes caused by the hemodynamic response that accompanies neural activity. Due to differences in optical absorption between different forms of hemoglobin, PAI has the potential to distinguish oxy-hemoglobin (HbO2) and deoxy-hemoglobin (HbR) levels in blood, as well as simultaneously distinguish increased blood flow, without the use of external contrast agents. Compared to purely optical based imaging modalities, PAI is less invasive, as the skull does not have to be opened, and has superior resolutions while keeping high optical contrast. Its resolution (~100µm), fast image acquisition, relatively low cost and portability make the technique competitive compared with fMRI and PET/SPECT. In our study we use PAI to monitor changes in neural activation in the barrel cortex of young rats (Rattus norvegicus; Wistar unilever strain, 6 weeks old) during stimulation of the whiskers. The scalp is removed, but the skull is kept intact, restricting the level of invasiveness. For the photoacoustic measurement we used the Twente double-ring sensor, as described in [1]. First C-scans (3D image) were made of the brain, with and without stimulation of the whiskers, to locate blood vessels and the barrel cortex. After localizing a region of interest, one-dimensional (depth) images (A-scans) of the tissue were made in this area at three different wavelengths (750nm, 800nm, 850nm), making it possible to calculate HbO2/HbR concentration change and blood flow changes. The C-scans show changes in activation and blood flow, with strongest effect in the central blood vessel and in the barrel cortex region. The time traces of oxy- and deoxy-hemoglobin show nice correlations with the stimulation block design used, with an initial increase in deoxy-hemoglobin, followed by an increase of oxy-hemoglobin. These findings are in line with our understanding from other techniques such as fMRI and show the potential of this new technique in the field of small animal neuro-imaging. REFERENCES [1] J. Jose, S. Manohar, R.G.M. Kolkman, W. Steenbergen and T.G. van Leeuwen, "Imaging of tumor vasculature using Twente photoacoustic systems", J. Biophoton. 2, No. 12, 701–717 (2009).

(SEMI) AUTOMATIC SOFTWARE TOOLS FOR THE THERAPEUTIC MANAGEMENT OF AS
Volkan Tuncay, Wisnumurti Kristanto, Peter van Ooijen, Matthijs Oudkerk
Abstract: Purpose: Aortic Stenosis (AS) is one of the most common native valve diseases in the western society with increasing prevalence among the ageing population.[1]. The aortic valve area (AVA) is the indicator of AS and as such, the AVA can assist the physician to diagnose AS. The area of the aortic annulus can be used to determine the implant size. Currently, a physical tool called

'sizer' is used to determine the size of the implant during surgery. Accurate preliminary knowledge of aortic annulus area could therefore reduce procedure time required for valve replacement. Currently, all measurements of AVA and aortic annulus are performed manually. Our purpose is to develop (semi) automatic software that can be used in the diagnosis and the surgery planning of AS. Material and Methods: A program was developed with Matlab® to peform the required segmentation semi-automatic. A combination of a number of well-known segmentation techniques such as thresholding, region growing and Gradient Vector Flow (GVF) snake algorithm was used for the semi-automatic segmentation. There are two major steps of the program. Firstly a binary image is created by region growing and thresholding which are used to determine the AVA and aortic annulus respectively. The binary images are later processed with GVF snake algorithm to outline the desired area. The user has to place arbitrary amount of seed points inside the aortic valve opening area to draw the initial contour which will expand to boundaries of the opening area. One seed point is sufficient to determine the area of the aortic annulus. The program was tested on 21 CT images of calcified aortic valves. Three blinded observers manually segmented the images. These results were compared with the semi automatic segmentation. Results: The aortic annulus was successfully segmented in all images and the semi-automatic AVA segmentation was successful segmented in 17 out of 21 images. Conclusion: In conclusion, in most cases the semi-automatic segmentation of AVA is feasible although some improvements are still required to achieve the same result in studies with lower image quality. Refernces: 1. Iung B, Baron G, Butchart EG et al (2003) A prospective survey of patients with valvular heart disease in Europe:the euro heart survey on valvular heart disease. Eur Heart J 24:1231–1243

DESIGN AND PROTOTYPE DEVELOPMENT OF A WEARABLE NEURAL STIMULATOR SYSTEM WITH FLEXBILE WAVEFORM ADJUSTMENTS

Marijn van Dongen, Wouter Serdijn, Robert van Spyk, Christos Strydis, Georgi Gaydadjiev

Abstract: Many pathologies find their origin in the central or peripheral nervous systems. In any cases drugs have limited effectiveness and/or they cause unwanted side effects. functional electrical stimulation of the nervous system using implantable neural stimulators has the potential of becoming a major source of treatment for a wide variety of diseases. When comparing existing neurostimulators to their cardiac muscle equivalents (cardiac pacemakers), they seem to offer surprisingly limited functionality. An electrical feedback mechanism is missing and patient comfort is drastically reduced due to the need for subcutaneous wires between the chest and the brain. Furthermore neural stimulators have their own specific needs, especially when it comes to waveform flexibility. To address the problem of neural tissue habituation and to better mimic the natural neural signals, a wide variety of stimulation waveforms is required. This, in contrast to existing devices which are able to generate only square shaped waveforms. Our project aims to offer the technological push, which will pave the way for more effective, efficient and patient friendly neural stimulation. A novel stimulator design has been proposed [1] with a focus on waveform flexibility and low power consumption. Rather than current based stimulation, this stimulator controls the fundamental quantity of interest directly: the electric charge. As a first step towards the Integrated Circuit (IC) realisation of the complete system a Printed Circuit Board (PCB) version is developed. This wearable stimulator is able to generate an infinite set of waveforms, while still assuring charge cancellation and current limit protection for safety purposes. It consists of an analogue frontend, which conveys the stimulation signals into the tissue. The frontend is connected to an ATMega168 microcontroller on the Arduino BT platform. The system is controlled using a Google Android smartphone application using secure Bluetooth connection. In this way, the unconstrained number of device adjustments can be very easily configured by practicing physicians who will simply use a mobile phone. The use of the PCB prototype neurostimulator will provide medical researchers with the possibility to take advantage of the full potential of neurostimulators, much more than with existing devices. It is envisioned that our project will lead to improved and more effective treatment methods for a wide variety of neural disorders.

PROPHYLACTIC VERTEBROPLASTY DECREASES THE FRACTURE RISK OF ADJACENT VERTEBRAE

Rene Aquarius, Jasper Homminga, Allard Hosman, Nico Verdonschot, Esther Tanck

Abstract: Osteoporosis, a metabolic disorder, induces the risk of a vertebral wedge fracture. Wedge fractures of the vertebrae are associated with pain and spinal malalignment. An initial vertebral fracture changes the loading direction on adjacent vertebrae from the normally seen axial load to a more shearing load. As osteoporotic vertebrae are more prone to failure under such shearing loads, the chance of subsequent fractures is increased. We hypothesized that the previously found increased fracture risk of intact but osteoporotic adjacent vertebrae, can be reduced when these adjacent vertebrae are prophylactically injected with bone cement. Thirty one vertebrae were harvested from four fresh frozen cadaveric spines. The posterior elements were resected at the pedicles in order to facilitate placement in our testing setup. Twenty one vertebrae were used in our previous study into the effect of the shearing loads, while 10 were used in this study into the effects of prophylactic vertebroplasty. These 10 vertebrae underwent a bipedicular, prophylactic vertebroplasty (injected bone cement volume: 8.2 ml (SD=2.1 ml)). Both endplates of each vertebra were cast in bone cement and the vertebrae were subsequently placed under 20° in our testing setup. The 20° loading angle was chosen in order to mimic the off-axis loading that vertebrae adjacent to a fractured one experience. Each vertebra was loaded at a rate of 2 mm/min while force and displacement were registered at 10 Hz, allowing the calculation of failure load (the highest peak) and stiffness (the linear elastic part of the curve). These data were compared to data from our previous experiment, in which 21 unfilled vertebrae were loaded either perpendicular to the endplate (n=11, 0° group) or under an angle of 20° (n=10, 20° group). The measured failure load and stiffness of all 3 groups were compared using a one-way ANOVA (with an LSD post hoc test) with the significance level set to $p < 0.05$. We previously found that the mean failure load of the 0° group (2845N, SD=591N) was significantly higher ($p=0.02$) than that of the 20° group (2163N, SD=670N). For the prophylactically treated group, that was loaded under 20°, the mean failure load was 2850N (SD=703N). Thus comparable to the mean failure load of the 0° group ($p=0.99$), but significantly higher than that of the 20° group ($p=0.03$). We previously found that the mean stiffness of the 0° group (3979N/mm, SD=928N/mm) was significantly higher ($p<0.01$) than that of the 20° group (2478N/mm, SD=453N/mm). For the prophylactically treated group, that was loaded under 20°, the mean stiffness was 3156N/mm (SD=582N/mm). Thus lower than the stiffness of the 0° group ($p=0.01$), and higher than that of the 20° group ($p=0.04$). In conclusion; a prophylactically augmented osteoporotic vertebra is better able to withstand the off-axis loads that occur after the initial fracture compared to an unfilled vertebra. However, before advising prophylactic filling of adjacent vertebrae, the risks that are associated with the currently available techniques for vertebroplasty should be assessed and eliminated.

TEN REASONS FOR APPLYING STATIC BALANCE IN BIOMECHANICAL ENGINEERING

Just Herder

Abstract: In biomechanical engineering, solutions that work well in industry cannot always be applied Oftentimes, dedicated technology is needed, such as static balancing, i.e. creating constant system potential. Advantages of statically balanced systems in biomechanical appliations, including the following ten. 1 Compensation of undesired forces. A first feature is the possibility to eliminate the influence of previously existing undesired conservative forces. 2 Energy-free motion. Statically balanced systems can be moved with no operating effort in the presence of considerable conservative forces, such as gravity. 3 Full energy exchange. Balanced mechanisms make possible the full energy exchange between several energy storage devices, with no operating effort during quasistatic motion. 4 Improved information transmission. Elimination of undesired forces also improves feedback since forces are transmitted without distortion through the mechanism. 5 Energy-free force control. The forces in the fixed points of the springs in a balanced mechanism can be put to use, e.g. clamp function. As the clamping force can be controlled without any operating effort, i.e. infinite force amplification can be achieved. 6 Elimination of backlash. Forces can be added in a neutral equilibrium configuration so that they have no influence on the force transfer function, yet eliminate backlash by prestress. 7 Zero stiffness. Another feature of statically balanced systems is that they possess zero stiffness, which makes them useful in vibration isolation. 8 Neutral buoyancy. By using gravity equilibrators, forces due to gravity are compensated. This allows zero-gravity simulation, for instance for space research applications. 9 Improved performance. In general, precision of operation is enhanced if loading characteristics are reduced. Smaller actuators are needed (if any), the construction can become more light-weight, control is simplified, power consumption and heat rise are reduced. 10 Inherent safety. Finally, the fact that statically balanced mechanisms are in equilibrium when unactuated presents a form of safety. In conclusion, static balancing has, while based on a single premise of constant potential energy, different feaures that each, or in combination, are particularly profitable in biomechanical engineering, and also have application potential elsewhere. REFERENCES [1] J.L. Herder, Theory, Conception and Design of Statically Balanced Spring Mechanisms, Ph.D. Thesis, Delft University of Technology, 2001.

INTERACTIONS OF ELECTROMAGNETIC FIELDS AND THE HUMAN BODY: TOOLS FOR PREDICTING INDUCED ABSORPTION, CURRENTS AND TEMPERATURE RISE

Jurriaan Bakker, A.C. Christ, E. Neufeld, Maarten Paulides, N. Kuster, Gerard van Rhoon

Abstract: Humans are exposed to electric and magnetic fields that vary in both time and location. Electromagnetic fields (EMF) are for example generated by the transmission of electricity, by domestic, industrial and medical applications and in telecommunications and broadcasting. During the last century, the use of electrical devices and therefore the exposures of humans to electromagnetic fields have increased. Especially the rapid increase in mobile phone use and more recently, wireless technologies has led to a growing concern among the public about potential negative health effects. EMF are exploited also in a number of medical applications such as Magnetic Resonance Imaging (MRI) and Hyperthermia devices in the treatment of cancer. The dielectric properties of the human body are heterogeneous and consequently, the propagation of EMF and interaction with human tissues is complex. Therefore, sophisticated tools are required to model the human body characteristics and predict the propagation and interaction of EMF with human tissues. In this study, we demonstrate numerical tools to model the interaction of EMF with human tissues efficiently and accurately. The first tool iSEG is used to quickly and easily generate a set of anatomical whole-body models from high-resolution MRI or CT data. Fully automatic and interactive segmentation techniques are combined to process 2D image data into 3D electromagnetic and thermal models. The poser package allows for deformation of the anatomical models to mimic realistic body postures. The second tool

SEMCAD-X is used as a platform to simulate the complex electromagnetic interactions and to predict the induced absorption, currents and temperature increase. The Extremely Low Frequency (ELF) toolbox provides an advanced electro-, magneto- and quasi-static full wave Finite Element simulator. The parallel Finite Difference Time Domain (FDTD) solver enables fast transient, broadband and harmonic simulations by using hardware acceleration on either multi-core CPU or GPU clusters. The thermal solver is a standalone application that is coupled to the EM simulations. It uses an improved Pennes Bioheat Equation, with discrete vessel modelling, temperature dependent tissue properties, tensorial heat diffusion, flow patterns, convective and mixed Neumann and Dirichlet boundary-conditions. The solvers in SEMCAD-X are interfaced by Python, and MATLAB scripts for fast and efficient generation of the simulation configurations and analysis of the results. This unique combination and connection of the described tools enables fast and accurate EMF exposure and medical technology simulations, such as 1) brute-force examinations of various EMF exposure scenarios, 2) field optimization of medical devices, 3) hyperthermia treatment planning and 4) safety assessments of whole-Body MRI with implants or pacemakers and 5) design of transmit and receiver coils.

CRPS-INDUCED VASOMOTOR DYSFUNCTION MEASURED BY PULSE TRANSIT TIME
Minke Kortekaas, Sjoerd Niehof, Marit van Velzen, Robert Stolker, Frank Huygen
Abstract: INTRODUCTION. Complex Regional Pain Syndrome (CRPS) is a complication after surgery or trauma. In CRPS bloodflow can be altered due to vasomotor dysfunction (VMD). VMD can be caused by autonomous dysregulation (efferent mechanism) and/or endothelial dysfunction (afferent mechanism). Clinically, it is difficult to distinguish between these mechanisms. Therefore we need a reliable and objective method to assess the cause of VMD, with as goal a more mechanism based treatment. Pulse Transit Time (PTT) is the time between contraction of the heart (R-wave on ECG) and arrival of the resulting arterial pulse wave in the fingertips (photoplethysmography (PPG). PTT is a measure for arterial compliance. By using temperature mediated vasomotor response (TMVR) and flow-mediated dilation (FMD), it should be possible to determine the underlying mechanism. METHODS. In this study 37 patients with CRPS (IASP-criteria) will be compared with 37 age- and sex matched healthy volunteers. Exclusion criteria are cardiovascular disease, diabetes and hematopoietic diseases. Data were obtained using the MP100 Biopac® system with 16-bit data acquisition. Three external ECG leads (ECG100C amplifier, Biopac®) were placed to acquire a 2nd lead for R wave detection together with photopletysmographic sensors (TSD200 and PPG100C amplifier, Biopac®) on the index fingers of both hands. Data were sampled with 2 kHz using the AcqKnowledge 3.7.3 version software (Biopac®). To measure the efferent mechanism, a temperature (cold and heat) pain stimulus is applied with the TSAII (Thermo Sensory Analyzer, Medoc®, Israel). This evokes a vasoconstrictive TMVR. Due to the vasoconstriction, the diameter of the bloodvessel decreases and the PTT becomes shorter. The afferent mechanism is tested with FMD. After a baseline measurement, we induce arterial occlusion of the upperlimb of 5 minutes. The occlusion causes reactive hyperemia resulting in endothelial dependent vasorelaxation. In response to this, the bloodvessel dilates and the diameter of the bloodvessel increases resulting in an increased PTT. The PTT-change from baseline and the recover time to baseline will be determined. The values are compared to the contralateral arm. During the perturbations the PTT is measured together with the Laser Doppler Flow and videothermography. RESULTS. Preliminary results show no difference in PTT in healthy volunteers between both arms after TMVR and FMD. The PTT after FMD in the CRPS-involved arm is altered compared with healthy volunteers. In the CRPS-involved arm the PTT first decreases and recovers to baseline. In healthy volunteers the PTT first increases and then returns to baseline. CRPS-patients show a TMVR at a lower threshold in the involved arm. CONCLUSION. PTT has potencial as a diagnostic tool in CRPS with VMD. However, more patients need to be included before definite conclusions can be drawn.

PREDICTING PARAMETER DEVELOPMENT IN PROGRESSIVE DISEASES
Christian Tiemann, Joep Vanlier, Jeroen Jeneson, Peter Hilbers, Natal van Riel
Abstract: To improve our understanding of progressive diseases it is important to study the causal molecular adaptations in underlying biological systems that drive their onset. Traditionally, biological systems are being studied by experimentally comparing two different states: a control state and a perturbed state [1]. Although this gives valuable information about begin and end stages, one would like to understand which molecular adaptations are collectively responsible for the change of state and how they progress in time. Here, we propose a computational approach to obtain this information from a system evolving from phenotype A to a phenotype B. Fundamental in the approach is the development of a mathematical model, representing the biological system of interest. Data of the initial state (phenotype A) is used to parameterize the model by performing a large-scale search to obtain a collection of parameter sets describing the initial state. Parameter alteration trajectories, required to describe the change in phenotype, are determined by interpolating the data from phenotype A to phenotype B in a step-wise manner, whilst simultaneously reoptimizing the parameters to describe the interpolated data. The approach was employed to study metabolic consequences of liver X receptor (LXR) activation, which is a promising drug target to treat atherosclerosis [2]. We were able to quantitatively integrate data of wild-type C57BL/6J mice into a consistent model and identified a collection of parameter sets describing this state. Furthermore, trajectories of parameter alterations, describing the change from wild-type C57BL/6J mice to LXR activated C57BL/6J mice, were determined. Several parameters change significantly and consistently from the initial to the altered phenotype and are in good agreement with gene expression data [1, 3]. [1] A. Grefhorst et al., “Stimulation of lipogenesis by pharmacological activation of the liver X receptor leads to production of large, triglyceride-rich very low density lipoprotein particles”, Journal of Biological Chemistry, Vol. 277, pp. 34182-34190, (2002). [2] M.H. Oosterveer et al., “The Liver X Receptor: control of cellular lipid homeostasis and beyond Implications for drug design”, Progress in Lipid Research, Vol. 49, pp. 343-352, (2010). [3] J.W. Chisholm et al., “The LXR ligand T0901317 induces severe lipogenesis in the db/db diabetic mouse”, The Journal of Lipid Research, Vol. 44, pp. 2039-2048, (2003).

SELECTIVITY AND RESOLUTION OF ELECTRICAL STIMULATION OF FINGER MUSCLES FOR GRASPING SUPPORT
Ard Westerveld, Alfred Schouten, Peter Veltink, Herman van der Kooij
Abstract: Grasping objects is an important function in daily life. Grasping becomes difficult or even impossible for a large number of patients with motor dysfunction (like spinal cord injury, hemiplegia due to stroke, Duchenne muscular disease, Multiple Sclerosis and many others). Electrical stimulation of arm and hand muscles can be a functional tool for these patients. Sufficient stimulation of finger and thumb musculature can support or train natural grasping function [1]. Yet it remains unclear how different grasping movements can be selectively supported by electrical stimulation and what the optimal electrode positions are, i.e. the positions with the highest selective range. The goal of this study is to find the optimal electrode locations for the forearm and hand musculature in individual healthy subjects and to assess the intersubject variability. In addition, we investigated if the optimal electrode locations depend on wrist posture [2]. The three main muscle groups involved in grasping were selected. A virtual stimulation grid was placed over each muscle belly to select the cathode locations. The evoked forces in individual fingers were measured. Stimulation thresholds and selective ranges were determined for each subject. Optimal stimulation locations were compared between subjects and between different wrist postures. In all subjects selective stimulation of middle finger extension and thumb flexion was possible. Selective stimulation of index and ring finger extension was possible in most cases. Selective stimulation of the little finger was achieved in only 4 of 10 subjects. The variability of optimal stimulation locations between subjects was large. The influence of wrist posture was also highly variable between different subjects. The size of selective ranges, is highly variable between different fingers and between different subjects. Furthermore the grid points which allow selective stimulation at all differ enormously between subjects. Concluding, this study demonstrates that the optimal stimulation locations for finger and thumb muscles are highly variable between subjects. Within the design of grasping prostheses and grasping rehabilitation devices, the variability of optimal stimulation points should be taken into account. The results of our study facilitate the optimization of such designs and favour a design which allows individualized stimulation locations.

ACOUSTIC WAVE FIELD MODELING FOR ULTRASOUND BREAST CANCER DETECTION
N. Ozmen Eryilmaz, P.M. van den Berg, A. Gisolf, Frans Vos, Nicole Ruiter, Koen van Dongen
Abstract: Mammography and Magnetic Resonance Imaging (MRI) are the best known scanning methods used for detecting breast cancer. However, they have some limitations. Mammography gives poor detection for dense breast, uses ionizing radiation which increases the risk to get cancer and is uncomfortable for patients. MRI is expensive and has a long examination time. On the other hand, ultrasound is cost-effective, painless, harmless, and provides good detection for dense breast. In collaboration with the Karlsruhe Institute of Technology (KIT), we work on the development of new ultrasound imaging techniques to improve the ultrasound scanning quality by providing more detailed characterization of the breast tissue. In order to assess the efficiency of the imaging algorithms, they are first tested on synthetically measured, noise free data. Since there is no commercial software available which can handle such complex and large spatial domains of interest, this data is computed using in-house developed software. In this software, a conjugate gradient scheme is used to solve the integral equation which describes the propagation and scattering of the acoustic wave field in an inhomogeneous medium in the temporal Fourier domain. In this way, it accounts for multiple scattering and allows for large three-dimensional problems. To test the accuracy of the algorithm, we have compared the outcome with an analytical solution for an acoustically penetrable sphere illuminated by a time harmonic plane wave field. This research is supported by the Dutch Technology Foundation STW, which is the applied science division of NWO, and the Technology Programme of the Ministry of Economic affairs. REFERENCES [1] J.T. Fokkema and P.M. van den Berg, Seismic Applications of Acoustic Reciprocity. Elsevier, Amsterdam, 1993. [2] H.A. van der Vorst, “Bi-cgstab: A fast and smoothly converging variant of bi-cg for the solution of nonsymmetric linear systems,” SIAM J. Sci. Stat. Comput., vol. 13, no. 2, pp. 631-644, 1992.

AUTOMATIC TRACKING OF MAXIMAL RESPONSES FOR EXCITABILITY TESTING OF HUMAN PERIPHERAL NERVES
Leonard van Schelven, Rolf Struikmans, Dirk Straver, Hessel Franssen
Abstract: Threshold Tracking [1] measures excitability of human peripheral nerves in vivo. Here, excitability is defined as the electrical current required for activating a group of axons in a nerve. This is monitored by measuring the compound muscle action

potential (CMAP), recorded from a muscle innervated by the nerve. Excitability can be affected by nerve conditioning, for instance by cooling, prolonged nerve activity or electrical conditioning currents. In a typical Threshold Tracking setup, the stimulus strength is adapted automatically by feedback control, to obtain a constant CMAP size. In that way, the effect of conditioning on excitability, that is: on the required stimulus strength, can be studied. An important advantage of Threshold Tracking is that it estimates effects on a fixed group of axons. A known problem with this is that activation of the same axons does not always generate the same CMAP. For instance after prolonged muscle contraction, the CMAP size can change. In such situations, a better estimate of the excitability is obtained by not tracking to a fixed CMAP, but to a fixed fraction of the maximal CMAP [2]. The actual maximal CMAP must then be monitored, which is normally done by giving additional stimuli at a 'maximal current' level, set manually for a measurement session. In a pilot study we found that this method is insufficient because the maximal CMAP cannot be well monitored using a fixed 'maximal current'. We therefore developed software (MaxTracker) that, by feedback, dynamically adapts the 'maximal current' which it uses to monitor the maximal CMAP. The MaxTracker can be implemented in the widely used QTRAC software for Threshold Tracking [3]. The MaxTracker may provide new information on the effect of conditioning and may help to approximate the goal of exciting the same group of axons at all times. We will present the design of the MaxTracker, and discuss some of the trade-offs involved. We will demonstrate its functioning and usefulness by measurements before and after a period of maximal voluntary muscle contraction. REFERENCES [1] H. Bostock, K. Cikurel, and D. Burke. Threshold tracking techniques in the study of human peripheral nerve. Muscle Nerve 21 (2):137-158, 1998. [2] D. Burke, M. C. Kiernan, and H. Bostock. Excitability of human axons. Clin.Neurophysiol. 112 (9):1575 -1585, 2001. [3] Software by H. Bostock (UCL, London), available from Digitimer Ltd., Hertfordshire, England

COMPARISON OF MULTI-UNIT MICRONEUROGRAPHY AND MODEL SIMULATIONS OF THE MUSCLE SPINDLE
Karin de Gooijer-van de Groep, Leonard van Schelven, Herman van der Kooij, Liam Oey, Frans van der Helm
Abstract: With microneurography (MNG) a Tungsten needle electrode is inserted in a nerve. With this technique it is possible to record afferent and efferent signals in vivo in humans. There are two ways to perform MNG: single-unit and multi-unit MNG. With multi-unit MNG several fibers are recorded. It is therefore expected to record a mixture of different fibers which makes is difficult to classify these fibers. However, the technique is easier to execute than single-unit MNG. In this research we used multi-unit MNG to study whether we could measure signals coming from the muscle spindles. We compared the effect of velocity and movement amplitude on MNG responses with model simulations of the muscle spindle. 5 subjects were examined with ramp-and-hold perturbations during MNG measurements (24-30 yr, 2 male). Wrist movements were imposed using a robot manipulator. Multi-unit MNG signals were obtained from the radial nerve of the left upper arm. Passive wrist movements were performed with different velocities and amplitudes. Ramp-and-hold perturbations (flexion and extension) were used with three different velocities (1.5, 3.0 and 5.0 rad/s) and three different amplitudes (0.06, 0.10 and 0.14 rad), resulting in nine different combinations of velocity and amplitude. Each combination of velocity and amplitude was repeated five times. Perturbations were applied in random order in five sessions of about 90 seconds. The five MNG signals of each combination were averaged. The nine combinations were used to study the sensitivity of the muscle spindles to velocity and amplitude. They were compared to model simulations using the model of Mileusnic et al. 2006. When increasing the velocity of the perturbation when lengthening the extensor muscles, all subjects showed an increased response in the MNG. This was e.g. showed by higher peak responses and an increase of baseline MNG after each perturbation. These changes were less clear when increasing the amplitude of the perturbation. A different response was visible when shortening the extensor muscle. Instead of the expected steady baseline or decreased MNG activity there was an increase of the MNG signal when shortening. No baseline increase was found. Model simulations showed similarities in peak response and baseline changes when lengthening the muscles. This was not the case when shortening the muscle. Multi-unit MNG can be used to study the behavior of muscle spindles to passive ramp-and-hold perturbations. Model simulations showed similarities with the measured MNG signals, confirming the assumption that muscle spindle signals were measured, but interference of other nerve signals cannot be excluded. That might explain the unexpected MNG response on muscle lengthening. In future experiments we will analyze ramp-and-hold perturbations during constant force. REFERENCES [1] Mileusnic MP, Brown IE, Lan N, Loeb GE. Mathematical models of proprioceptors: I. Control and transduction in the muscle spindle. J Neurophysiol 2006; 96: 1772-1788.

AN EASY TO USE INSTRUMENT POSITIONER FOR MINIMALLY INVASIVE SURGERY
Jesse Bosma, Joris Jaspers
Abstract: Holding an endoscope or other static instruments during Minimally Invasive Surgery (MIS) can be a rather fatiguing, cumbersome and somewhat boring job. Usually an assistant is in charge of this task, so that the surgeon has no direct control over his viewing direction. This can easily result in communication problems and disturbance of the surgeon's eye-hand co-ordination. Moreover, it is hard to obtain a sustained stable endoscopic view. A few systems with an endoscope positioning function have been assessed in the past, but most of these systems are expensive, bulky, complex or not intuitive to use [1]. At University Medical Center Utrecht, we have developed a new positioning device for endoscopic instruments. It features a simple construction that aims at user friendly operation of the device. This includes easy one-handed operation of the device and a slender design that minimizes the interference with other instruments in the sterile field. The positioning system actually fixates all degrees of freedom of the trocar and the instrument going through it simultaneously, in a drag 'n drop manner. Engaging the operating button of the device removes the fixation of the degrees of freedom of trocar and instrument, releasing the button freezes the instrument in the desired position immediately. The operating button of the system can easily be attached to the instrument to be fixated, which improves the intuitive way of interacting with the device even more. Current status is a demonstrator proof of principle and a patent application. We are planning to develop a prototype for clinical evaluation in the near future. Additionally, we hope to be able to improve the opportunities of solo surgery, which is possible with single handed operated passive holders [1]. Moreover, passive holders perform as well as active holders and as well as human control [1,2] The instrument positioning system is a user friendly, single- hand operated device that helps to provide a stable endoscopic view and may be able to benefit solo surgery.

THE RATIO BETWEEN TISSUE AND SCAFFOLD DURING TISSUE DEVELOPMENT IN CARDIOVASCULAR TISSUE ENGINEERING
Rashna Soekhradj-Soechit
Abstract: ABSTRACT Background: Cardiovascular tissue engineering aims to develop living heart valve and blood vessel replacements with growth and remodeling potential. Such replacements are based on autologous vascular cells and synthetic rapid degrading scaffold material. During development of such tissues, the ratio between tissue and scaffold, in terms of weight contribution, changes continuously. It is important to quantify this ratio to compare the tissue composition of engineered tissues with their native counterparts or with tissues that are engineered using other scaffold materials. In this study, we present a method that enables quantification of the ratio between tissue and scaffold in engineered tissues. The feasibility of this method is demonstrated by quantifying this ratio over time in engineered tissue strips. Methods: PGA/P4HB scaffold strips (n=12) were seeded with human vascular cells using fibrin as a cell carrier and cultured up to 4 weeks. The engineered tissue strips were analyzed after 1 (n=3), 2 (n=3), 3 (n=3) and 4 (n=3) weeks of culture to determine the ratio between tissue and scaffold at each time point. The strips were freeze-dried and weighed to determine the total dry weight (DW1), which represents the weight of both tissue and scaffold. Subsequently, the dried strips were digested with papain and the undissolved remnants were freeze-dried. The weights of these remnants represent the weight of the remaining scaffold (DW2). To test whether tissue was completely removed after digestion, a BCA assay was performed. The ratio between tissue and scaffold was calculated by (DW1-DW2)/DW2 at each week of culture. Results: The BCA assay confirmed that the tissue was removed after digestion and implies that the remnants after digestion represent scaffold material only. The total dry weight of the engineered strips remained constant in the first 3 weeks, after which a drop in total dry weight was observed. A similar trend was shown for the weight of the scaffold remnants over time. The relative amount of tissue in the engineered strips increased from 38% after 1 week to 76% after 4 weeks, while the relative amount of scaffold decreased from 62% after 1 week to 24% after 4 weeks. Conclusion: We demonstrated a method that enables quantification of the ratio between tissue and scaffold in engineered tissues based on the dry weight before and after protein digestion. In addition, we showed that the ratio between tissue and scaffold changes dramatically during culture. Furthermore, this methodology will allow comparison of tissue composition of engineered tissues with their native counterparts or with tissues that are engineered using other scaffold materials.

HEALTH-2007-2.4.5-10: UNDERSTANDING AND COMBATING AGE RELATED MUSCLE WEAKNESS "MYOAGE".
Astrid Bijlsma, Carel Meskers, M.D.W. van der Bij, Andrea Maier, Jurriaan de Groot, Erwin de Vlugt
Abstract: Sarcopenia is literally a universal, age-related loss of muscle mass. Its onset and dimension are muscle dependent and heterogeneous. It can occur as early as 30 years of age and result in a loss of about 30-50% of the muscle mass by the age of 80 years (1). Sarcopenia causes a decline in muscular strength and is associated with negative clinical outcomes such as physical disability, cognitive decline and mortality (2). Despite its clinical importance, the pathofysiological processes leading to sarcopenia as well as the subsequent functional decline are largely unknown. A complex range of factors may contribute to sarcopenia, i.e. neuropathic, hormonal, immunological and nutritional factors (3). Lack of exercise is also found to be a significant risk factor for sarcopenia, so that there may be a negative spiral of sarcopenia, physical inactivity, sarcopenia. There are indications that sarcopenia not only comprises a quantitative loss of muscle strength, but also a qualitative decline in muscle function. The exact relation of sarcopenia to not only muscle strength, but also power and work, in which also the neural system as the muscular controller plays a significant role, is yet largely unknown. Within the FP7 framework MYOAGE program, 525 subjects are being recruited in five European centers. The cohort comprises both highly active and sedentary cognitively healthy subjects between 70 and 80 years old and a young group (18-30 years). Muscle physiological and morphological parameters, physical and cognitive performance measures as well as biomaterial are being collected for each participant. In Leiden as one of the recruitment centres, we also include 1) a closed loop system identification approach to discern intrinsic tissue characteristics from performance of the neural controller around the wrist joint (4), 2) a 7 Tesla MRI scan of the brain and 3) muscle biopsies. A combined epidemiological, muscle physiological, biological and control engineering approach together with state of the art imaging is a very powerful tool to unravel causes and effects of sarcopenia.

Outcome will be important to define targeted intervention and prevention strategies. REFERENCES [1] Abellan van KG. Epidemiology and consequences of sarcopenia", J Nutr Health Aging 2009; 13(8):708-12. (2009) [2] Beenakker KG, Ling CH, Meskers CG, de Craen AJ, Stijnen T, Westendorp RG, Maier AB. Patterns of muscle strength loss with age in the general population and patients with a chronic inflammatory state. Ageing Res Rev 2010; 9(4):431-6. [3] Narici MV, Maffulli N. Sarcopenia: characteristics, mechanisms and functional significance. Br Med Bull 2010; 95:139-59. [4] Schouten AC, De Vlugt E, Van der Helm FCT. Design of a torque-controlled manipulator to analyse the admittance of the wrist joint. J Neurosci Meth. 2006; 154:134-141.

DESIGN OF A PASSIVE EXOSKELETON WITH ARTIFICIAL TENDONS
Wietse van Dijk, Herman van der Kooij, Edsko Hekman
Abstract: Many of current exoskeletons lack applicability due to high power requirements[1]. Different studies suggested that passive exoskeletons with bio-inspired design are capable of reducing the metabolic cost of walking[2, 3]. Van der Bogert introduced an inspiring idea: using artificial tendons. This idea was not yet implemented in an exoskeleton. This study presents an exoskeleton that uses artificial tendons. The effect of the artificial tendons on the energy cost of walking is determined in an experiment. The aim of this study is to show that the metabolic cost of walking can be reduced with an exoskeleton that uses the artificial tendons. Artificial tendons: The purpose of the artificial tendon is to redistribute energy over the gait cycle and over the joints. The artificial tendon is an elastic cable that spans over the hip, knee, and ankle joint. The artificial tendon has an offset from the joint centres. The offset makes it possible to exert a torque around the joints and lets the artificial change length if the leg moves. The elastic behaviour of the tendon makes it possible to store energy. The amount of energy stored in the artificial tendon depends on the stiffness and the elongation of the tendon. Optimization: The joint offsets, the spring stiffness, and the rest length are optimized to minimize the joint power. The optimization shows that the joint powers could be reduced by 40%. Two important assumptions are made in the optimization: the cost function sufficiently scales with the metabolic cost, and the artificial tendons do not change the walking kinetics. Prototype: The optimization results are used for the design of a prototype for a passive exoskeleton. Besides the rotations in the sagittal plane, the exoskeleton allows for ab- and adduction of the leg, this makes it possible to walk on a treadmill. The exoskeleton is adjustable for different users. The weight of the exoskeleton is approximately 12 kilograms. Human experiments: Preliminary tests were performed with the prototype. Three walking conditions are tested: normal walking (no exoskeleton), exoskeleton walking with the artificial tendons, and exoskeleton walking without the artificial tendons. Normal walking is the most energy efficient. While walking with the exoskeleton, the heart rate and the oxygen consumption decrease if the artificial tendons are attached. Conclusion: Both in simulation and in experiment the artificial tendons showed promising results. Implementing passive elastic elements in exoskeletons can have a positive effect on the power requirements, and is worth considering for any new exoskeleton. REFERENCES [1] Ferris, D. P., Sawicki, G. S., & Daley, M. A. (2007). A physiologist's perspective on robotic exoskeletons for human locomotion. International journal of HR: humanoid robotics, 4(3), 507-528. [2] van den Bogert, A. J. (2003). Exotendons for assistance of human locomotion. BioMedical Engineering OnLine, 2(1), 17. [3] Dollar, A. M., & Herr, H. (2008). Lower Extremity Exoskeletons and Active Orthoses: Challenges and State-fo-the-Art. IEEE Transactions on Robotics, 24(1), 144-158

SINGULAR VALUE DECOMPOSITION AND CHANGE OF BASIS IMPROVE THE INVERSE SOLUTION IN ELECTROCARDIOGRAPHY
Matthijs Cluitmans, Ronald Westra, Ralf Peeters
Abstract: Reconstructing heart-surface potentials from body-surface potentials is known as the inverse problem of electrocardiography. [1] This problem is ill-posed: the solution is very sensitive to small disturbances in the set of body-surface potentials. Therefore, regularization techniques are applied to impose additional constraints on the solution, for example with Tikhonov methods or Generalized Minimal Residual (GMRes) methods. [2, 3] In this study, Singular Value Decomposition (SVD) is applied to incorporate new constraints. For a given torso-heart geometry, the potential vectors Φ_H on the heart surface and Φ_B on the body surface are commonly modelled to be related by a transfer matrix Z, depending on conductivity of the medium: Φ_B= Z Φ_H. SVD here yields Z=UDV^T, in which the columns of matrix U form a basis for the potential patterns on the body surface, the columns of V form a basis for the potential patterns on the heart surface, and diagonal matrix D relates those bases. [4] Note that the diagonal entries of D represent the level of geometrical transferability of basic potential patterns at the heart-surface to basic potential patterns at the body-surface. When the diagonal entries of D are arranged in decreasing order, the first columns of U and V (the pairs of left and right singular vectors of Z) represent the best transferable basic potential patterns. Truncating D removes the basic potential patterns that are not transferable well. We have used a realistic heart-body geometry and its corresponding transfer matrix for testing purposes. Applying the truncated SVD to the transfer matrix allows to reconstruct heart-surface potentials from the (noisy) body-surface potentials in a robust way. Preserving only 10% of the singular values yields a relative error (RE) of 0.25 between the original and reconstructed heart-surface potentials. This performance is comparable to the solution given by the GMRes (RE = 0.26) and Tikhonov (RE = 0.25) regularization techniques. SVD can also be applied to the time-series of noisy body potentials Φ ̃B=PΛ_B Q^T, as in [5]. The columns of P serve as a new basis for the body surface potentials. Rewriting the measured potentials in this new, truncated basis yields a small improvement (RE=0.21). Further improvements are gained by applying the SVD also to a simulated training set of realistic heart-surface potentials Φ ̃H=SΛ_H T^T, which is new. This combined approach results in a relative error of 0.10, outperforming traditional regularization methods by 60%. Including Λ_B and Λ_H in the new bases can alter the outcomes even further (RE=0.08 for including Λ_H, RE=0.17 for including Λ_B). Methods need to be developed to select the optimal number of singular values to preserve in each decomposition and to determine the restrictions of the use of a training set of heart-surface potentials for reconstructing unexpected potential patterns. In conclusion, application of SVD in solving the inverse problem of electrocardiography is greatly improved by truncation of basic potential patterns determined by geometry, measurements and expected potential patterns. REFERENCES 1. Rudy, Y. and B.J. Messinger-Rapport, The inverse problem in electrocardiography: solutions in terms of epicardial potentials. Crit Rev Biomed Eng, 1988. 16(3): p. 215-68. 2. Ramanathan, C., et al., Noninvasive electrocardiographic imaging (ECGI): application of the generalized minimal residual (GMRes) method. Ann Biomed Eng, 2003. 31(8): p. 981-94. 3. Ghosh, S. and Y. Rudy, Application of L1-Norm Regularization to Epicardial Potential Solution of the Inverse Electrocardiography Problem. Annals of Biomedical Engineering, 2009. 37(5): p. 902-912. 4. Golub, G. and C. Reinsch, Singular value decomposition and least squares solutions. Numerische Mathematik, 1970. 14: p. 403-420. 5. Damen, A.A. and J. van der Kam, The use of the singular value decomposition in electrocardiography. Med Biol Eng Comput, 1982. 20(4): p. 473-482.

GRASP CONTROL FOR MYOELECTRIC HAND PROSTHESES
Bart Peerdeman, Stefano Stramigioli, Sarthak Misra
Abstract: A patient with a unilateral amputation will always prefer to use their remaining hand to perform most actions. The prosthesis is only used when support of the main hand is required. Therefore, the prosthesis should not aim to replace all functionality of the missing limb, but simply provide support and ease of use. Grasping is one of the most basic functionalities of the human hand, and is the main component of a large number of bimanual actions. A prosthesis that is easily controlled to perform various grasps can therefore be very helpful. In this research, various control systems are tested and evaluated. To test the control systems, a biomechanical model has been developed [1]. Its design is based on the structure of the human hand, having five fingers with three flexion/extension degrees of freedom (DOFs) and one abduction/adduction DOF each. Several different high- and low-level control systems are tested on the model, and evaluated with regard to the functional requirements described in [2]. The control system can be divided into two parts: the high-level control system, which determines the actions to be performed from the user's input signals, and the low-level control, which determines joint and actuator torques based on the desired finger positions. When a grasp type is selected, the prosthesis should move the fingers to the right position to begin the grasp. This process is called preshaping. After preshaping is completed, the hand can be positioned around the object to be grasped, and the grasp can be closed. The grasp execution system should allow control of both closing and opening of the hand, as well as the application of additional force on a held object. After setpoints have been issued by the high-level control system, the low-level control needs to determine the correct motion and dynamic behavior of the fingers. The fingers should move to their end position quickly, naturally, and should react compliantly to any obstructions. The high-level grasp control is tested by executing lateral, tripod and cylindrical grasps controlled by simulated EMG input. Position control, impedance control and intrinsically passive control are each implemented and tested by way of a simple grasping task for each grasp type. The improved performance of the latter control methods is demonstrated by grasping tests with objects of varying size, shape and stiffness. After the validity of both the high- and low-level systems is demonstrated in software, the completed control system is tested on the UB hand IV prosthesis prototype [3]. REFERENCES [1] B. Peerdeman et al. A modeling framework for control of myoelectric hand prosteses. In Proceedings of the 32rd Annual International Conference of the IEEE Engineering in Medicine and Biology Society, pp. 519-523, Buenos Aires, Argentina, September 2010. [2] B. Peerdeman et al. Myoelectric forearm prostheses: State of the art from a user requirements perspective. (Under review) [3] G. Berselli et al. Integrated mechatronic design for a new generation of robotic hands. In Proceedings of the International IFAC Symposium on Robot Control, pp. 105-110, Gifu, Japan, September 2009.

MECHANICAL CHARACTERIZATION OF HUMAN ATHEROSCLEROTIC PLAQUES AND THE UNDERLYING VESSEL WALL
Renate Boekhoven, Marcel Rutten, Marc van Sambeek, Frans van de Vosse
Abstract: Introduction The possibility to identify the risk of rupture of a carotid plaque will have tremendous impact in clinical decision making. Currently, selection of candidates for surgery is based mainly on Duplex ultrasonography, where only patients with severe carotid artery stenosis (≥70%) undergo endarterectomy. Only one out of six symptomatic patients with a 70-99% stenosis benefits from a carotid intervention1. Therefore, identification of patients at high risk of stroke (i.e. with unstable/vulnerable plaques, at an early stage would permit timely intervention while substantially reducing unnecessary treatment of stable plaques. Aim To investigate whether stress distribution and composition of the plaque and underlying vessel wall are important factors to be determined for plaque rupture prediction to become feasible. Materials & Methods A pilot study was performed to investigate the possibility to put relevant mechanical loads into effect to human atherosclerotic carotid arteries, harvested from endarterectomy.

Each intact carotid endarterectomy sample was fixed in an organ bath and was loaded with a pulsatile pressure. Results The experimental set-up enabled the access of ultrasound imaging with a 2D linear array probe, still tracking the vessel wall including calcifications needs further attention. Also preparation of the samples requires improvement, because frequent damage in the vessel wall caused the samples to be leaky. As a consequence the maximum pressure obtained so far was 40 mmHg. Discussion The carotid endarterectomy samples are suited for this study, leakage problems are to be solved. The experimental set up will be adjusted to enable rotation of the sample in order to obtain a 3D image, and to overcome the acoustic shadowing effect due to sample calcifications. Strains in the vessel wall and plaque will be obtained from the ultrasound RF data using dedicated software (ESAOTE). Project outline Non-linear mechanical properties of the atherosclerotic arteries will be estimated with an inverse numerical model (based on the fibre-reinforced model2), using the ex vivo loading and histology data as input. With these mechanical properties a finite element method will be developed predicting the stability of the plaque using a patient specific geometry as input.

ASSESSMENT OF DAILY-LIFE DYNAMIC INTERACTIONS BETWEEN HUMAN BODY AND ENVIRONMENT USING MOVEMENT AND FORCE SENSING ON THE INTERFACE

Henk Kortier, Peter Veltink

Abstract: The physical interaction between the human body and environment is important in many situations: In physical labor, interactions need to be performed within safe limits of body loading. In rehabilitation, people need to relearn functional motor tasks and interact with mobility support devices. In sports, motor tasks are trained to the ultimate, maximizing force and/or endurance and optimize coordination. The dynamic interaction between the human body and environment can be assessed in terms of forces and movement at the interface. We have shown that power transferred and work done can be estimated using signals from force and movement sensors at the interface [1]. It should be noted that these force and movement quantities also provide information about the dynamic characteristics of the environmental load as well as of the human body. In general, both bodies are physically coupled and therefore interact in a closed loop. Hence, the relation between effort (forces) and flow (velocities) variables gives information about the joint dynamics. This study describes a method to estimate load dynamics during the execution of daily life tasks. In many motor tasks, the central nervous system (CNS) applies feed-forward control, using learned patterns. The contribution of state feedback (visual/proprioceptive/reflexive) is significantly less when a certain task has been performed multiple times. We hypothesize that force and movement measured at the interface provide information about load dynamics for this class of tasks, since the load is effectively moved under open-loop conditions. An instrumented handle has been used to measure forces and accelerations on the interface of human hand and a mass and spring load. Both mass and spring loads have been repeatedly transferred between two positions. During the mass load experiments mass was estimated within 4% difference with the real measured value. Estimated damping and stiffness were neglectable. In the case of a spring load, stiffness was estimated within 3% of the actual value. We conclude that simple load dynamics can indeed be identified during motor tasks that involve learned feed-forward controlled motor patterns. We propose that limited information of body dynamics can be obtained when load dynamics suddenly changes (for example when releasing an object that is thrown). In addition, task performance may be quantifiable from force and movement information.

COMPUTER-AIDED UTLRASOUND (CAUS) TO DETERMINE LIVER FAT CONTENT APPLIED IN AN ANIMAL MODEL AND IN PATIENTS

Gert Weijers, Johan Thijssen, Geert Wanten, Marinette van der Graaf, Chris de Korte

Abstract: ABSTRACT Related to our Western World life style, obesity is a growing problem. In obese people, fat is not only accumulated in a subcutaneous fat layer but also in the liver (steatosis). Steatosis is one of the main causes for developing diabetes type-2 in obese populations. Patients on Home Parenteral Nutrition (HPN) are also at risk for developing hepatic dysfunctioning due to steatosis. For this reason, a cost effective, non-invasive technique for the assessment and follow-up of hepatic fat content is highly needed. The authors developed and tested a quantitative ultrasound technique [1] for the staging of steatosis using Ultrasound Tissue Characteristics (UTC) parameters from B-mode images. This method was validated with an extensive animal study in 151 cows [2]. In that study, both transcutaneous and intra-operative images could be analysed. Since also biopsies were taken, correlation with histology could be made. High predictive values (ROC, Area Under the Curve: AUC=0.97; Sensitivity: 88% and Specificity: 90%) were found for the classification of the liver fat content into several risk groups. Recently, the authors showed that removal of hepatic vessels by automatic Ultrasound (US) image segmentation [3] improved the predicted values in staging liver steatosis. Transcutaneous US was found to be a non-invasive, low-cost, quick, suitable and rather sensitive method for quantification of liver steatosis in hepatic livers. Currently the feasibility of this technique is being evaluated in human patients who are on Home Parenteral Nutrition (administrated at least 6 times per week). Presently, data have been obtained from six patients on HPN for 8 yrs (range 1-33). From each patient five independent US liver images were acquired using a Linear Array transducer (Sonos7500 with L11-3 transducer, Philips Medical Systems, Bothell, USA) at an inter-costal position. These images were analyzed using the CAUS protocol. In short: Linearization of the Look Up Table to yield pure logarithmic encoded echo levels and the expression of the gray levels in decibel. Estimation of and correction for the combined skin, fat and subcutaneous layer thickness and attenuation. Automatic segmentation for the removal of hepatic arteries and portal veins. Finally several Ultrasound Tissue Characterization (UTC) parameters; Mean echo level, Standard deviation of mean echo level, Signal to Noise Ratio, Attenuation Coefficient, Axial and Lateral speckle size (averaged values, slope and intercept of linear regression with depth) were estimated. The CAUS UTC parameter results were validated using an absolute quantification of liver fat concentration by proton Magnetic Resonance Spectroscopy (MRS, 3T Trio MR system, Siemens, Erlangen, Germany) at the same day. Positive and significant ($p<0.05$) correlations were obtained between several US parameters determined using CAUS and MRS liver fat content (Mean echo level r=0.85, Attenuation r=0.83, Lateral speckle size r=0.72). Consequently, CAUS may also have potential in staging and screening of hepatic steatosis in human liver, thus preventing taking biopsies. REFERENCES [1] J.M. Thijssen, A. Starke, G. Weijers, et al., Computer-aided B-mode ultrasound diagnosis of hepatic steatosis: a feasibility study, IEEE TUFFC 55, 1343-1354, (2008). [2] A. Starke, A. Haudum, G. Weijers, et al., Non-invasive detection of hepatic lipidosis in dairy cows with calibrated ultrasonographic image analysis, J Dairy Sci. 93, 2952-2965, (2010). [3] G. Weijers, A. Starke, A. Haudum, J.M. Thijssen, J. Rehage, C.L. de Korte. Interactive versus automatic ultrasound image segmentation methods for staging hepatic lipidosis. Ultrasonic Imaging, 32, 143-153, (2010).

SENSITIVITY OF MUSCULOSKELETAL MODELS TO FUNCTIONAL AND IMAGE-BASED SUBJECT-SPECIFIC SCALING

Vincenzo Carbone, Marjolein van der Krogt, Nico Verdonschot, Bart Koopman

Abstract: Musculoskeletal diseases and prosthetic revision operations concerning lower extremities represent a huge burden that increases rapidly with the aging population. For patients requiring major surgical interventions, procedures are still uncertain in outcome and have a high complication rate. The main objective of the EU-funded project TLEMsafe is to develop, validate and clinically implement an ICT-based patient-specific surgical navigation system that integrates modelling, simulation and visualization tools. This will offer surgeons a system to safely reach the optimal functional result for the patient and a user friendly training facility. The starting point is the recently developed Twente Lower Extremity Model (TLEM), based on the first comprehensive and consistent anatomical dataset, in which all relevant parameters are measured from a single cadaveric specimen [1]. The outcome of a musculoskeletal model is highly dependent on anatomical parameters and muscle properties [2]. Subject-specificity is essential in TLEMsafe to assess the patient's capacities. Geometrical 'linear' scaling, based on the subject's height and weight, is a commonly used method to represent different patients, but it might result in inaccuracies caused by inter-individual anatomical differences and co-variances between parameters. For these reasons, the anatomical dataset of TLEM will be personalized for every patient, extracting an individual parameter set based on medical imaging (MRI/CT) measurements (listing bone geometry, muscle insertion points and cross sectional areas, etc.) and on functional kinematic and dynamic tests (listing overall muscle strength, joint centres, etc). In the present substudy of TLEMsafe, a sensitivity analysis will be performed to assess the effects of errors in functional and medical imaging measurements on the subject-specific model outcome. The objective is to quantify the effect of perturbing single muscle parameters, like insertion points and cross sectional areas, on the time histories of forces developed by all the muscles. This research will be performed initially for gait, and afterwards for more demanding tasks of daily living, like stair climbing or sitting down and getting up from a chair, in order to determine whether sensitivity depends on the task performed. The inter-individual variability of the most sensitive parameters will be analyzed, based on literature data and new cadaver measurements. The results of this sensitivity study will be very important for TLEMsafe, and for personalized musculoskeletal modelling in general, in order to develop a priority list of the parameters necessary as input for the subject-specific model, containing requirements for both functional and medical imaging measurements. ACKNOWLEDGMENT The TLEMsafe project is funded by the European Commission FP7 programme REFERENCES [1] M.D. Klein Horsman, et al., "Morphological muscle and joint parameters for musculo-skeletal modelling of the lower extremity", Clin Biomech 22, pp. 239-247, (2007). [2] C.Y. Scovil, J.L. Ronsky, "Sensitivity of a Hill-based model to perturbations in model parameters", Journal of Biomechanics 39, pp. 2055-2063, (2006)

MID-INFRARED SOLID-STATE LASER SYSTEMS FOR MINIMALLY INVASIVE SURGERY

Stefan Been, Herke Jan Noordmans, Ruud Verdaasdonk

Abstract: In 1995 it was demonstrated that targeting biological tissues with a mid-infrared Mark-III Free-Electron Laser (FEL) at wavelengths near 6.45 µm results in tissue ablation with minimal collateral damage and a substantial ablation rate, which is especially useful for e.g. neural & ophthalmologic surgery [1,2]. Based on these findings the European Union has granted a 3 year FP7 project to a consortium to develop advanced table-top solid-state photonic sources for this specific wavelength in the mid-IR spectral range, as a practical, reliable and cost-effective alternative to large-scale free-electron lasers (FELs). The ultimate goal of this project is to make this laser source a viable supplement to the existing medial laser assortment on the market. 4 work packages have been defined in this project. Material research [WP1]; Pump laser development [WP2], OPO development [WP3] and Verification [WP4] Each project partner is working one of more work packages to ultimately develop 4 OPO systems that will be compared to the existing FEL results. The visualisation and quantification experiments are being performed by the UMC Utrecht in collaboration with

the VU medical center to analyze the ablation parameters of these systems. Unique visualization techniques have been developed to study the interaction of various infrared laser wavelengths. Model and biological tissues are used to obtain a better understanding of the ablation mechanism and the contribution of physical processes such as shockwaves, cavitation, explosive vapor, tissue heating, thermal conduction and diffusion. Using a unique sub surface thermal imaging set up, Schlieren imaging and high speed imaging techniques a comparison among parameters such as energy, pulse duration and diameter of focus can be obtained [3]. At this point one of the four OPO systems in development is running stable at 6.45 µm with energy levels around the ablation threshold of tissue (1.2 mJ at 25 Hz).. We have obtained some preliminary ablation results with our imaging setups on this system, however the energy levels are still to low to verify these findings to the FEL literature results. Milestones of the coming project year indicate that the energy levels of the OPO systems will be around 5 to 10 mJ per pulse at repetition rates around 25 Hz. This will enable a decent comparison with existing laser sources and the FELs and explore its earlier mentioned future clinical applications.

THE ROLE OF INITIAL STRESS IN ATHEROSCLEROTIC PLAQUE MODELING
Lambert Speelman, Ali Akyildiz, Jolanda Wentzel, Anton van der Steen, Brigit den Adel, Louise van der Weerd, Wouter Jukema, Rob Poelmann, Harald van Brummelen, Frank Gijsen
Abstract: Stress analyses on atherosclerotic plaques are more and more performed with the ultimate goal of using stress as a diagnostic parameter for plaque rupture. Plaque models are in most cases based on in-vivo measurements and initial stress (IS), which is present due to the blood pressure at the time of imaging, is usually ignored [1,2]. The aim of this study is to identify the effect of IS on the stress results of realistic coronary plaque geometries. Twenty 2D plaque models were created based on histological data of three plaques in two diseased coronary arteries from a single patient. The diseased arteries were pressurized and fixed at 13.3 kPa before histological preparation and cross-sections of 5 micrometer were obtained. In the cross-sections, the lumen, the largest lipid core, the intima, and the media were manually delineated. Meshing and stress computations were done with Abaqus Standard 6.9. Neo-Hookean material models were used with commonly used parameters [1,2]. IS was computed using an in-house written python script, based on the Backward Incremental method as described previously in [3]. IS was determined up to a pressure of 13.3 kPa and thereafter, a peak systolic pressure of 18.6 kPa was applied. The peak plaque stress is compared to the peak stress as computed without IS. Including IS in the stress computations had a profound and disperse effect on the resulting peak stresses of the individual sections, with a change in peak plaque stress ranging from -40% to +28% (-3% on average). The change in peak cap stress ranged from -55% to +51% (-6% on average). The effect that IS has on the peak cap stress showed a relation with the cap thickness. Sections with a thin cap showed a general decrease in cap stress when IS was incorporated, while for thicker caps the cap stress increased. This may be caused by the suppression of the large deformations of thin caps, while this deformation is much smaller for thicker caps. Likely, the effect of IS is therefore larger for thinner caps than for thicker caps. The IS did change the relationship between the peak stress in the cap and various geometrical features in a quantitative way, but qualitative they stayed the same, either with or without IS. For both, peak cap stresses increased for thinner caps and thicker lipid pools, as was also found in earlier studies [1,2]. For future patient -specific rupture risk analyses, incorporating IS is indispensible in the stress analyses. To determine qualitative relations between stresses in the caps of atherosclerotic plaques and geometrical features of the plaques, IS may be omitted from the stress computations. [1] Finet et al., Arch Mal Coeur Vaiss. 100(6-7):547-53, 2007. [2] Ohayon et al., Am J Physiol Heart Circ Physiol. 295 (2):H717-27, 2008. [3] Speelman et al., J Biomech. 42(11):1713-9, 2009.

ENERGY LOSS AT REST AND IN EXERCISE CONDITION IN PATIENT SPECIFIC FONTAN GEOMETRIES
Rene Verhaart, Sjoerd Bossers, Willem Helbing, Jolanda Wentzel, Frank Gijsen, Frans van de Vosse
Abstract: Introduction - Most congenital heart disease patients with a single ventricle are treated with a Fontan procedure. In this 3-staged procedure the blood flow from the superior vena cava (SVC) and inferior vena cava (IVC) is directed toward the pulmonary arteries. One of the medical complications after this procedure is a decreased exercise capacity. It is suggested that the energy losses in the Fontan geometry play an important role in the decreased exercise capacity. Previous studies [1, 2, 3] that investigated this hypothesis used simplified geometries or do not use measured exercise flow for their patient specific CFD simulations. The aim of the current study is to apply patient specific flow measurements in patient specific geometries in order to determine the energy losses at rest and in exercise condition. Methods - In a group of five patients, rest and exercise flow measurements were performed in the SVC, IVC and pulmonary arteries using a phase contrast velocity-encoding MRI sequence. The exercise condition was mimicked by an intravenous administration of dobutamine. Furthermore, a method was presented to generate a 3D patient specific Fontan geometry from anatomical data obtained with MRI. The 3D patient specific Fontan geometry and the blood flow measurements in the same patient were used to perform a CFD simulation in both rest and exercise. The CFD simulation gives us the local pressure and velocity in the Fontan geometry from which the energy loss was computed. Results – Parallel streamlines were observed in the IVC and the SVC. At the anastomosis, the flow collides. Together with the abrupt change in the flow direction at the anastomosis, the colliding flow induces swirling flow patterns in both pulmonary arteries. The flow division as well as the swirl patterns in the two pulmonary arteries depended on geometrical details and the total flow rate. The dobutamine induced a slight increase in flow for all the patients (19%). This increase in flow had only a minor influence on the observed flow patterns. However, the energy loss changed significantly from 0.64 to 1.18 mW, an increase of 80%. Discussion and conclusion - The velocity patterns and energy losses for the five patient models varied greatly and depended on geometry and flow. The minor increase in flow due to the dobutamine induced a significant increase in energy loss. To further investigate and quantify the effect of flow and geometry on energy losses in Fontan patients, we need to extend this study to a larger series of patients. [1] Whitehead, K.K., et al., Circulation 2007; 116: I-165 - I-171. [2] Marsden, A.L., et al., Annals of Biomedical engineering 2007; 35(2): 250-263. [3] Dubini, G., Journal of Biomechanics 1996; 29(1), 111-121

AUTOMATIC IDENTIFICATION AND LOCALIZATION OF INERTIAL SENSORS ON THE HUMAN BODY
Dirk Weenk, Bert-Jan van Beijnum, Peter Veltink
Abstract: Human motion capture is used for many purposes like sports training and rehabilitation. In the last few years, inertial sensors (accelerometers and gyroscopes) in combination with magnetic sensors was proven to be a suitable ambulatory alternative to traditional human motion tracking systems based on optical position measurements, which are restricted to a bounded area. While accurate full 6 degrees of freedom information is available, these inertial sensor systems still have some drawbacks [1, 2]. All sensors have a unique location ID, i.e. each sensor has to be attached to a certain predefined body segment, and they have to be connected by wires. Another disadvantage is the fact that the relative positions and orientations of the sensors with respect to the segments are unknown, which has to be resolved by a sensor-segment calibration procedure. These drawbacks cause the set-up time of the current systems to be relatively large. The goal of this project is to develop a 'Click-On-and-Play' ambulatory 3D human motion capture system, containing a set of wireless inertial sensors which can be placed on the human body at random positions, because they will be identified and localized automatically. In this first study the automatic identification of the inertial sensors is investigated, i.e. the automatic assessment of the body segment to which each inertial sensor is attached. This is done during normal walking and under the assumption that all sensors are present and attached to the body segments correctly. This problem is considered a classification problem, i.e. the sensors are divided into several classes (the body segments). A typical classification system consists of a feature extractor followed by a classifier. Walking data was recorded from eleven healthy subjects using an Xsens MVN motion capture suit with full body configuration (17 inertial sensors). Subjects were asked to walk for about 5-8 seconds at normal speed. The magnitudes of the 3D acceleration and 3D angular velocity were calculated. Features as variance, mean, correlations between sensors and power spectra were investigated. As a classifier a decision tree was developed. For all sensors it could be determined whether or not they are on the same lateral side, but the absolute left and right identification is not possible based on merely the magnitudes of the 3D accelerations and 3D angular velocities. For eight of the eleven subjects all sensors were identified correctly and totally 90.4% of all the sensors were identified correctly (no left and right, but only ipsi-/contralateral identification). The next step is to look into the left and right identification, the identification during other daily-life activities, and the identification of a subset of the 17 sensors. Also automatic classification algorithms like Weka (Waikato Environment for Knowledge Analysis) will be used and compared with these first results. After the identification, the in-use estimation of orientation and position of the sensor with respect to the segment will be investigated. REFERENCES [1] D. Roetenberg, H. Luinge, and P. Slycke. 6 DOF Motion Analysis Using Inertial Sensors. In Proceedings of Measuring Behavior 2008 (6th International Conference on Methods and Techniques in Behavioral Research), pages 14–15, Maastricht, The Netherlands, August 2008. [2] H.M. Schepers, D. Roetenberg, and P.H. Veltink. Ambulatory human motion tracking by fusion of inertial and magnetic sensing with adaptive actuation. Medical and Biological Engineering and Computing, 48(1):27–37, 2010.

PLAQUE CHARACTERIZATION IN EX VIVO MRI EVALUATED BY DENSE 3D CORRESPONDENCE WITH HISTOLOGY
Arna van Engelen, Marleen de Bruijne, Stefan Klein, Harald Groen, Jolanda Wentzel, Aad van der Lugt, Wiro Niessen
Abstract: Rupture of instable carotid atherosclerotic plaques is one of the main causes of stroke. Evidence is present that vulnerability mainly depends on plaque composition. A large lipid-rich necrotic core (LRNC) covered by a thin fibrous cap is associated with a high risk of rupture, while fibrous tissue (FT) and calcifications (Ca) have a stabilizing effect. MRI has shown to be capable of imaging different components non-invasively. Automatic segmentation and quantification of plaque composition in MRI is therefore an important goal. Previously, plaque characterization methods were evaluated by manually matching 2D MRI slices to selected histological slices. In contrast, we train and evaluate a classification using 3D registration of histology to ex vivo MRI [1]. 3D registration is more objective than 2D methods, as it eliminates selection bias. In addition it allows accounting for differences in slice orientation between histology and MRI. For 12 patients plaque histology was obtained and manually segmented into LRNC, FT and Ca. Registration of ex vivo MRI (T1W, T2W, PDW and 3DT1W) with histology followed different steps using both rigid and deformable registration and involved several manual annotations. Classification was performed using linear (LDA) and quadractic (QDA) Bayes discriminant analysis for different feature combinations, and was evaluated in a leave-one-out manner. As features the intensity in

the four contrast weightings after different degrees of Gaussian smoothing, the distance to the lumen and outer vessel wall and derivatives in the x- and y-direction of the images with a medium degree of smoothing were used. The best overall accuracy (66%) was reached with LDA when all original and smoothed intensity images and the spatial features were used. Derivatives did not lead to a better accuracy. Good accuracy for Ca was reached, however, differentiation between FT and LRNC was more difficult. A possible explanation is that fibrous and necrotic tissue often occurs mixed, raising both difficulties in classification and in ground truth generation from histology. This research was supported by the Center for Translational Molecular Medicine and the Netherlands Heart Foundation (PARISk)

THE EFFECT OF CONDUCTION BLOCK AND FAILING MYOCYTES ON CARDIAC PUMP FUNCTION: TOWARDS A PATIENT-SPECIFIC MODEL

Esther Warnert, Evelien Hermeling, Nico Kuijpers

Abstract: Left Bundle Branch Block (LBBB) causes a delayed depolarization of the left ventricle (LV) of the heart. Therefore, asynchronous contraction of the left and right ventricle (RV) will occur, leading to a decreased pump function. On the other hand, LV dysfunction can also be caused by failing myocytes (FM) leading to prolonged action potential duration and decreased intracellular calcium concentration [1]. At present it is not possible to determine whether heart failure in a specific patient is mainly caused by LBBB, FM or a combination. The aim of this simulation study was to investigate the effect of LBBB, FM, and the combination on LV function, as determined by ejection fraction (EF), maximal change in LV ventricular pressure (dP/dtmax), and E/A ratio. A multi-scale computer model was developed that contained electrophysiology and calcium handling as well as cardiac mechanics and hemodynamics [2]. The pulmonary and systemic circulation were incorporated as well as inter- and intraventricular interaction [3]. With this model, a heart was simulated (Normal) in which septum, RV and LV free wall (LVfw) were simultaneously activated. Three simulations were performed with delayed depolarization of LVfw (LBBB), with a delay of 30, 60, and 90 ms, respectively. FM was simulated in three different situations: in the LVfw only, in septum only, and in both wall segments. In addition, three simulations were performed in which LBBB (delay 60 ms) was combined with the different cases of FM. Although the LV function worsened with increasing delay of activation, for all three LBBB simulations EF and dP/dtmax did not differ much from Normal. With increasing LVfw delay, E/A ratio diminished but remained within normal range. FM in the LVfw results in strong reduction in EF, dP/dtmax, and E/A ratio. In contrast, septal FM hardly affected LV pump function. Combining LBBB with FM resulted in substantially lower EF, dP/dtmax, and E/A ratio, being the lowest if FM was present in the LVfw and septum. In conclusion, LBBB alone has little influence on LV pump function. Similar results hold for septal FM. However, FM in the LVfw results in reduced LV function, which is even more reduced in the case of LBBB and FM in both wall segments. Our model is well-suited to simulate various gradations of LBBB and FM, such that a broad spectrum of heart failure patients can be modeled. REFERENCES [1] L. Priebe, D.J. Beuckelemann, “Simulation study of cellular electric properties in heart failure”, Circ. Res., Vol. 82, pp. 1206–1223, (1998). [2] N.H.L.Kuijpers, H.M.M. ten Eikelder, P.H.M. Bovendeerd, S. Verheule, T. Arts en P.A.J. Hilbers, “Mechanoelectric feedback as a trigger mechanism for cardiac electrical remodeling: A model study”, Ann. Biomed. Eng., Vol. 36, pp. 1816–1835, (2008). [3] J. Lumens, T. Delhaas, B. Kirn, T. Arts, “Three-wall segment (TriSeg) model describing mechanics and hemodynamics of ventricular interaction”, Ann. Biomed. Eng., Vol. 37, pp. 2234–2255, (2009).

MECHANO-ELECTRICAL FEEDBACK DURING LEFT BUNDLE BRANCH BLOCK AND CARDIAC RESYNCHRONIZATION THERAPY

Nico Kuijpers, Esther Warnert, Evelien Hermeling, Frits Prinzen

Abstract: ABSTRACT Cardiac Resynchronization Therapy (CRT) has emerged as an important therapy to improve pump function in patients with left bundle branch block (LBBB). Electrical excitation of the ventricles is synchronized by simultaneously pacing both ventricles. It is known that long-term asynchronous activation leads to a form of electrical remodeling, referred to as “T-wave memory”. T-wave memory is known to occur after a period of ventricular pacing, but its role during CRT is unclear. Evidence is growing that T-wave memory is induced by altered mechanical load, and thus is a form of mechano-electrical feedback (MEF) [1]. We hypothesize that this kind of MEF leads to local changes in the expression of L-type calcium channels, aiming at (partial) correction of local workload in the asynchronous ventricle, but also affecting local action potential duration (APD). The aim of the present simulation study was to investigate the effects of MEF during LBBB and CRT using a multi-scale computer model [2]. The model described cellular electrophysiology and calcium handling as well as cardiac mechanics and hemodynamics. Ventricular electromechanics was represented by a single cardiac fiber, while physiological pressure-volume loops were obtained by simulating the systemic circulation. LBBB was simulated by stimulating the fiber at one end (activation time 108 ms) and CRT by simultaneous stimulation at both ends (activation time 54 ms). During chronic LBBB, MEF lead to a reduction in local differences in external work as well as in dispersion of repolarization. During acute CRT, systolic function was acutely increased as was dispersion of repolarization. As a consequence diastolic function (reflected by E/A-ratio) was reduced. With chronic CRT, dispersion of repolarization decreased and diastolic function improved. We conclude that MEF may lead to an increase in dispersion of repolarization during the early phase of CRT, which may lead to impaired diastolic function and to ventricular arrhythmia. REFERENCES [1] D. Jeyaraj, L.D. Wilson, J. Zhong, C. Flask, J.E. Saffitz, I. Deschênes, X. Yu and D.S. Rosenbaum, “Mechanoelectric feedback as novel mechanism of cardiac electrical remodeling”, Circulation, Vol. 115, pp. 3145̄ 3155, (2007). [2] N.H.L. Kuijpers, H.M.M. ten Eikelder, P.H.M. Bovendeerd, S. Verheule, T. Arts and P.A.J. Hilbers, “Mechanoelectric feedback as a trigger mechanism for cardiac electrical remodeling: a model study”, Ann. Biomed. Eng., Vol. 36, pp. 1816́ 1835, (2008).

NAVIGATION IN LAPAROSCOPIC LIVER SURGERY – DETERMINATION OF LIVER SHIFT DUE TO PNEUMOPERITONEUM IN AN ANIMAL MODEL

Mariken Zijlmans, Thomas Langø, Anna Rethy, Christiaan van Swol

Abstract: Precise laparoscopic liver resection requires accurate planning and visualization of the important anatomical structures like blood vessels and tumors. Navigation based on preoperative images partly overcomes the general drawbacks of minimally invasive surgery, like reduction of free sight and lack of dexterity and tactile feedback, giving a good overview for planning of the procedure. However, the usefulness of preoperative images is limited in laparoscopic surgery and liver surgery in particular, seeing that the liver is shifted due to heartbeat, respiratory motion, the pneumoperitoneum, and surgical manipulation. The research group in Trondheim is developing a navigation system incorporating laparoscopic ultrasound to cope with changes in the anatomy during surgery.[1] A live animal model with tumors has been established to develop the navigation system.[2] An important aspect of such a system is the value (accuracy) of guidance based on preoperative data after insufflation. In this study we quantify the liver (tumor) shift due to pneumoperitoneum. Five multimodal tumor models [2] were injected in a porcine liver, and 3D cone beam CT-images were acquired intraoperatively at varying levels of insufflation pressure (0, 6 and 12 mmHg). Tumor translation between pre- and post-insufflation images was determined manually in three orientations by subtracting absolute coordinates of the center of the tumors. In case of a 6 mmHg insufflation pressure, average tumor translation was 0.2±0.5 mm in right-to-left (RL) direction, 15.4±1.6 mm in anterior-to-posterior (AP) direction, and 14.4±0.6 mm in caudal-to-cranio (CC) direction. For insufflation with a pressure of 12 mmHg average tumor translation was 2.1±0.7 mm in RL direction, 21.1±1.5 mm in AP direction, and 28.2±1.3 mm in CC direction. Tumor translation due to the pneumoperitoneum seems significant; values are in the same order of magnitude as translations due to breathing. However, results are based on one animal only, so more animal trials are planned to improve statistics. Moreover, the small standard deviations suggest rigid body translation of the volume defined by the tumor centers. Our current work focuses on changes in the shape of both the tumors and the liver, to investigate possible deformation of these volumes, including rigid and deformable registration. REFERENCES [1] Solberg et al. Navigated ultrasound in laparoscopic surgery. MITAT. 2009; 18(1); 36-53 [2] Rethy et al. Development of a multimodal tumor model for porcine liver. J Gastrointest Surg. 2010; July 24 (epub ahead of print)

WEARABLE HUMAN BODY POSTURE MEASURING SYSTEM

Par Dunias, Paul Willems, Anmin Jin, Andy Statham

Abstract: ABSTRACT In many medical applications, especially the orthopedic setting, ambulatory, monitoring of human joint angles could be of substantial value to improving rehabilitation strategies and unraveling the pathmechanics of many degenerative joint diseases (e.g. knee osteoarthritis). These measurements allow monitoring of daily activity patterns, joint angles and walking patterns, which could be of use in adjusting the applied therapy depending on the results measured. The measuring system/method introduced in this paper is meant for monitoring joint angles for instance knee joint which was monitored as the most relevant to pathologies of this nature. In more complex situations, for example with lower back pain prevention and/or rehabilitation, the level of bending in all directions of the lower back and the corresponding velocity could also be monitored preventing situations that should be avoided occurring by giving direct feedback to the user. SENSOR Single Sensor: Measuring bending in our setting is based on the change of electrical inductance of a very simple coil (a loop of a conductive wire). It appears that the inductance of a coil changes as the form of the coil changes. It is these elements that vary when the coil bends and thus consequently changes the inductance correspondingly. The wire used in this sensor is very flexible and thin and integrated in a carrier e.g.. knee brace, t-shirt, strap etc. A typical sample of the validation results show accuracies of less than 2 degrees. An extended description of the validation procedure and the corresponding validation results of this specific single bending sensor are reported in [1] and [2]. Multiple Sensor: A combination of the aforementioned single bending sensor can be used in the case of measuring more complex human joints, i.e. shoulder, wrist etc. Not only joints but also body posture i.e. torso, can be measured using a number of single bending sensors. Suppose a human body part, the lower back for example, which should be measured in terms of three angles (flexion-extension, lateral flexion-extension and rotation). Using a carrier, in this case a shirt, it was possible to attach a number of wire-loops on strategic positions around the body. Measuring with a multiple bending sensor consists of the following steps (a) calibration or modeling the single bending sensors separately, (b) calculating the body posture based on the readings of the single bending sensors. CONCLUSIONS A single bending human joint angle sensor system is presented. The measuring accuracy of ±2 degrees gives unique and sufficient basis for clinical ambulant applications. In case of more complicated body moving parts (shoulder, trunk etc.) a

combination of single bending sensors may be used to measure the relevant degrees of freedom of the body part under consideration. The accuracy results are for forward-backward bending and side bending very promising (<2 degrees). REFERENCES [1] J.L. Riskowski, A.E. Mikesky, R.E. Bahamonde and D. B. Burr, “Design and Validation of a Knee Brace With Feedback to Reduce the Rate of Loading” Jornal of Biomechanical Engineering, vol. 131, August 2009. [2] K. Meijer, R. Gransier, P. Dunias, P. Deckers, N. Guldemond, P. Willems, L. van Rhijn , “ Determination of Gait Kinematics with a “Smart” Knee Brace A Validation Study”, to be appear at 6th World Congress of Biomechanics.

THE OPERATION ROOM OF THE FUTURE, USE ANALYSIS AND DEVELOPMENT OF SCENARIOS TO IMPROVE FUTURE USE
Joris Jaspers, Yvo Pluymakers
Abstract: In 2004 the UMC Utrecht installed as one of the first hospitals in the Netherlands a dedicated Operating Room (OR) for Minimally Invasive surgery (MIS). This OR1-suite (Karl Storz) was aimed as a fully integrated multi-speciality surgical suite for MIS, which allow monitoring, access and networking of the OR equipment, as well as the acquisition, storage and display of image, patient data during the endoscopic procedure. A central user interface should allow efficient, simplified operation and online clinical images. Due to the system integration, the handling of complex equipment was aimed to considerably simplified, procedure times should decrease and operative risk could be reduced through simplified device operation. After years of experience working in this integrated operating theatre, the general impression was that the system was not used to its full potential and not all claimed functionality was used or working. Therefore we analyzed the current usage of this OR and compared it with its potential use through a threefold approach: inventarisation of potential use, observing current usage and a questionnaire on the requirements of the surgical team. In addition the usability of the OR 1 system installed in the UMC Utrecht was analyzed using a heuristic analysis. We found that the acquired integrated OR is not used to its full potential: • Ergonomics and working space were improved due to the flexible and easy positioning of equipment and multiple screens placed on ceiling arms. • Access, central control and networking of the MIS equipment were only partly used, due to lack of training and non-optimal user interface. • Communication and integration of patient data and imaging were not used, due to incompatible communication standards and the lack of proper data infrastructure. Based on our analysis, recommendations and design challenges have been composed to stimulate efficiency and safety in the operating room. We designed four modular use scenarios; varying from an OR with optimal image distribution for ergonomic use, to a complete integration with network, control and communication functions. This approach could help hospital staff to research their needs and formulate their demands before acquiring an integrated OR, so that the future OR-of-the-future will be used to its full potential.

SPRING-LIKE ANKLE FOOT ORTHOSES REDUCE THE ENERGY COST OF WALKING BY TAKING OVER ANKLE WORK
Daan Bregman, Vincent de Groot, Carel Meskers, Jaap Harlaar
Abstract: In patients suffering from multiple sclerosis (MS) and stroke gait is often limited by a reduced ability to push off with the ankle. To enhance the reduced ankle push off, energy-storing, spring-like carbon-fiber Ankle Foot Orthoses (AFO) can be prescribed. These AFOs store energy at the start of the stance phase, and return this energy at the end of the stance phase. It is expected that the energy returned by the AFO normalizes the ankle push off, and consequently reduces the high energy cost of walking. However, increases in ankle push have not been reported while wearing spring-like AFOs, whereas these AFOs have shown to decrease energy costs[1]. The aim of this study is to evaluate the mechanical functioning and the energy costs of walking with spring-like AFOs. We aim to gain insight in the mechanical performance of the AFO during walking, based on its mechanical characterization[2] In 10 MS and stroke patients we determined the metabolic energy cost of walking, 3D kinematics, joint powers, and joint work while walking with and without the AFO. We determined the mechanical characteristics of the AFO[2], and used this information to calculate the separate kinetics of the AFO and the patient while walking with the AFO. We found a significant decrease of 9.8% in energy cost when walking with the AFO. The total net work remained unchanged. However, the total amount of work performed by the patient was reduced by 9.6% when walking with the AFO, because the AFO accounted for 60% of the ankle work. In contrast to our expectation, the decrease in energy cost when walking with a spring-like AFO is not induced by an augmented net ankle push off, but by the AFO partially taking over active ankle work. The results of this study refine the understanding of the functioning of AFOs, which is expected to lead to a more personalized AFO prescription, and thereby a higher benefit for the patient in the future. REFERENCES [1] Danielsson & Sunnerhagen J Rehabil Med (2004) 36 165-168 [2] Bregman et al. Gait & Posture (2009) 30 144-149

STUDY OF ELECTRODE DESIGN AND OPTIMISATION FOR COCHLEAR IMPLANTS
Nishant Lawand, Paddy French, Jeroen Briaire, Johan Frijns
Abstract: Cochlear Implant (CI) is an electronic device to restore hearing to person who is deaf or severely hard of hearing. The important issue with the CIs is the electrode design and its placement in the cochlea. In the auditory nerve, potentials are induced due to electric currents which are transmitted to the brain. The commercial cochlear electrode arrays available are hand assembled and the wire bundles used are limited in electrode count (16-24), due to their large size relative to the size of the scala tympani (ST). Fabricating these electrodes by Silicon micromachining techniques potentially offers many advantages over the traditional fabricating method. These include: 1) deeper insertion to detect lower frequencies; 2) increased operating efficiency; 3) improved insertion techniques to avoid damage; and 4) Reduced cost due to batch fabrication [1]. Electrode fabrication processes and its complexity vary accordingly to the implant purpose, the location and the encapsulation procedure. Silicon allows us to fabricate these electrodes in micrometre range. For neural extracellular recording there are various methods of electrode fabrication which includes gluing together the shanks of the metal wire electrodes, connecting glass insulated micropipette electrodes, and depositing thin films on silicon substrates, which yield good multichannel recordings [2]. There are various technologies developed for fabricating silicon electrode arrays that are used for stimulating and recording the signals in the auditory prosthesis. The probes fabricated by U. Michigan use integrated circuitry on the back end of the substrate, polysilicon site conductors and Iridium Oxide (IrO) stimulating electrodes, and gold pads at the back end of the electrode as an external interface. The microprobes make use of a high-boron doped etch-stop to create micro needles [3]. The aim of this work is to investigate and explore fabrication techniques for electrodes used in Cochlear implant and to optimize the fabrication process. Different geometries and configurations for the contact electrodes are being investigated for safe stimulation of the neurons. To improve guidance during surgery, position sensors into the electrode will ease the process and also cause less trauma to the patient. The fabricated electrode along with its stiffness must also be flexible enough to obtain deep insertion in the cochlea and have a modiolus hugging feature to position the contact sites as close as possible to the neurons to ensure stimulation signal transmission to the auditory nerve.

ANATOMICAL PARAMETERS FOR MODELLING THE WRIST AND HAND
Judith Visser, DirkJan Veeger, Frans van der Helm
Abstract: A musculoskeletal model of the hand and wrist can facilitate insights into the functioning of the human hand and can be an aid in surgical decision making. Therefore a 3-D complete model of the hand and wrist is being developed. The model will be an extension to the Delft Shoulder and Elbow Model (DSEM) [1], resulting in the first complete upper extremity model. The purpose of this study was to collect the morphological parameters for building the hand and wrist model. Parameters include the 3-D locations of joint rotation axes of the forearm, wrist, thumb and finger joints, muscle attachments, trajectories, wrapping surfaces, volumes, pennation angles, fiber lengths and tendon lengths. One left arm upper extremity specimen was obtained from a fresh frozen cadaver (female 71 years old). A 3-D position tracking system (Optotrak Certus, NDI) was used to collect data of the anatomical landmarks and muscles. Custom made rigid marker clusters with 3 tracking markers each were fixated to the distal phalanges (5x), metacarpals (5x), ulna, radius, and humerus. Anatomical landmarks and muscle geometry were digitised using a marker pointer. Kinematic data were collected during passive motions of the segments around each of the individual joints. The anatomical data are being implemented in the hand and wrist model. Data for all muscles are available, and will be published for the scientific community world-wide. The joint rotation axes for all joints are calculated based upon the instantaneous axes. Based on these data, the inverse- and forward dynamic linked segment model of the hand is constructed via a similar approach as the DSEM [1]. The model consists of 22 rigid bodies, where the carpal bones are modelled as one segment, and other bones are modelled as individual rigid bodies. The model has 27 degrees of freedom at the joints, and 46 muscles which are modelled as multiple segments. In this project, an extensive and complete anatomical data set for the hand was collected. Geometrical data on the muscles are combined with physiological data about their size, morphology and composition. Thus far, the data set seems to be rather complete, and is in the process of being implemented in the first version of the biomechanical hand and wrist model. REFERENCES [1] Van der Helm, F.C., "A finite element musculoskeletal model of the shoulder mechanism", J Biomech,. Vol. 27(5), pp. 551-69, (1994). mechanism", J Biomech,. Vol. 27(5), pp. 551-69, (1994).

EVALUATION OF THE OPTICAL QUALITY OF RIGID ENDOSCOPES IN CLINICAL PRACTICE
Rens Wientjes, Herke Jan Noordmans
Abstract: To assure the optical quality of rigid endoscopes in clinical practice, a test bench has been developed to measure the illumination pathway using a LED and photo cell and the viewing pathway using a LCD generated test pattern and high resolution camera. By storing the results into a database, changes in quality can be followed over time. In this paper the results are presented of three and a half year of measurement at the central sterilization department after cleaning and before sterilization. In total 1053 measurements were performed on 227 rigid endoscopes of 44 different types. The accuracy of the measurements with the test bench proved to be within 5% for the illumination fibers and within 20% for the image contrast test which is ascribed to the intensity fluctuations of the LCD screen. The clinically used endoscopes appeared to degrade slowly and their lifetime, based on reaching 20% of their initial quality, was estimated at 2 to 8 years. We expected thinner and longer endoscopes to have a shorter lifetime, but we did not find a relation between these parameters. As expected brand new endoscopes have a better quality compared to clinically used endoscopes of the same type. Endoscopes returned from repair were generally better than used endoscopes but could not be

restored to the quality of new endoscopes. Remarkably, the quality of some repaired endoscopes dropped quickly within the first months after clinical use. In our measurements there was no compensation for the number of times the scope is used, cleaned, sterilized or the total time of usage. The use of a test bench to monitor the optical quality of endoscopes over time shows to be a valuable investment that will contribute to the quality of patient treatment. More research is required to reveal the cause of degradation and improve the significance and accuracy of the measurements. REFERENCES [1] H.J. Noordmans, S. Kruit, P. Stroosnijder, H. vd Brink, R.M. Verdaasdonk, “Quantitative assessment of degradation of the optical quality of rigid endoscopes in clinical practice”, Proc. of SPIE Vol. 6849, 68490K, (2008). [2] Rapportage van de projectgroep MICADO, “Kwaliteitsborging van Instrumenten en Apparatuur gebruikt bij Minimaal Invasieve Chirurgie”, June 2008, www.wibaz.nl.

MEASURING SHOULDER ANGLES USING THE MMAAS: A WEARABLE IMU-BASED DEVICE FOR MOTION AND MUSCLE FUNCTION ASSESSMENT

Alessio Murgia, Vincent Kerkhofs, Hans Savelberg, Kenneth Meijer

Abstract: Using motion capture (MOCAP) technologies during clinical assessment of movement impairments can lead to more objective evaluations and more informed therapeutic decisions. At present MOCAP technologies using micro-electromechanical systems (MEMS) are portable but only offer limited support for upper limb clinical analysis and are not designed to measure upper limb motion and muscle synergies simultaneously and in real-time. We have developed a wearable MOCAP system, the Motion and Muscle Ambulatory Activity System (MMAAS), which allows real-time wireless capturing of upper limb movements and EMGs in a single unit. The system consists of a 5-channel inertia measurement unit (IMU) module (100 Hz sampling) and an 8-channel EMG module (up to 2 kHz sampling). In this study we report on the initial assessment of shoulder movements during functional activities. Three healthy subjects wearing the MMAAS performed upper limb movements following a predefined protocol. Ten repetitions were performed during 3 activities: hand to contralateral shoulder, reaching to the ipsilateral side and reaching to the contralateral side. A 6-camera (MX3+) Vicon® MOCAP system sampling at 100 Hz was used as golden standard. Data were compared using root mean square errors (RMSEs) and difference vs. mean diagrams. The shoulder active ranges of motion calculated from the MMAAS outputs were underestimated compared to those from the Vicon. RMSEs ranged from 15.3° (SE: 1.2°) for flexion/extension (SFE), to 22.1° (SE: 6.4°) for adduction/abduction (SAA), to 26.7° (SE: 5.9°) for internal/external rotation. The RMSEs for SFE and SAA were comparable to those found on the hip joint during gait for a commercial MEMS-based system [1]. The angular differences between Vicon and MMAAS could be attributed to misalignments between the sensor’s axes and the real anatomical axes, as well as to skin movement artifacts. An optimization procedure is being investigated to correct these errors while additional validation using Vicon markers on the MMAAS sensors is planned to quantify the skin movement artifacts. The wearable nature of the MMAAS and the clinical features offered in the software interface make the device suitable for monitoring motion and muscle synergies during robot-rehabilitation therapy. REFERENCES [1] T. Cloete and C. Scheffer, "Benchmarking of a full-body inertial motion capture system for clinical gait analysis," in Proc. 30th IEEE EMBS Conference, pp. 4579-4582, (2008).

VALIDATION OF MRI BY ACCURATE MATCHING WITH HISTOLOGY

Lejla Alic, Joost Haeck, Stefan Klein, Karin Bol, Wiro Niessen, Magda Bijster, Monique Bernsen, Marion de Jong, Jifke Veenland

Abstract: The aim of this work is to develop a methodology for establishing an accurate 3D relation between in vivo MRI and corresponding 3D histology. The key features of this methodology are: a standardized image acquisition (including an intermediate ex vivo MRI), the utilization of a reference plane, a dense histological sampling, non-rigid B-spline registration and the utilization of the whole 3D data sets. Tumor-bearing rats (CA20948) were imaged in vivo and ex vivo using a clinical 3T MRI scanner. After the MRI acquisitions, tumors were histologically processed. Registration of in vivo images with ex vivo tissue sections is complicated by the shrinkage and deformation of the tissue. Since we needed to correct for these deformations during the registration procedure, and correcting for severe deformations in one go would challenge the registration results, we divided the registration into four distinct steps: reconstruction of tumour 3D integrity in histology (1), registration of 3D histology stack to 3D ex vivo MRI (2), registration of 3D ex vivo MRI to 3D in vivo MRI (3), and concatenation of separate registration transformations (4). All steps are greatly facilitated by the definition of the reference plane1. This provides good initialization to exploit a three-step strategy of gradually increasing degree of freedom. We started as rigid registration, followed by affine transformation allowing for isotropic scaling to account for volume changes, and finalized by non-rigid refinement. The displacement field was parameterized using a third order B-spline model with mutual information of a 32-bin histogram as a similarity measure3. The evaluation of the registration accuracy based on two observers showed similar trends: the accuracy increased with increasing degrees of freedom, the RMS error decreased from 1.2 for the rigid registration to 0.8 mm for elastic registration. The evaluation of protocol accuracy shows that a 3D-registration approach when complemented by standardized methodology is essential to accurately align histology to in vivo MRI. REFERENCES [1] L. Alic, et al. Multi-modal image registration: matching MRI with histology, SPIE Medical Imaging (2010) [2] Klein, et al. elastix: a toolbox for intensity-based medical image registration. IEEE Trans Med Imaging, 29, 196-205. (2010) [3] D. Rueckert, et al. Nonrigid registration using free-form deformations: application to breast MR images. IEEE Trans on Medical Imaging 18:712-721 (1999)

AN ADDITIVE INSTANTANEOUSLY COMPANDING READOUT SYSTEM FOR COCHLEAR IMPLANTS

Cees-Jeroen Bes, Wouter Serdijn

Abstract: At the moment, about 30 million people worldwide are suffering from hearing loss. Most people are helped with a simple hearing aid that just amplifies sounds coming to the ear. However, if the hearing loss is too severe, these aids will not help. More than 100.000 people worldwide need a more complex device in order to let them hear again. A cochlear implant is such a device and is partially implanted inside the human body. Today’s implants are not able to let people hear sounds as people hear them with normal hearing. The main cause can be found in the stimulation accuracy of the auditory nerve fibres. To improve this accuracy, research should be performed in order to improve stimulation algorithms, increase the amount of electrodes and focus the stimulation field of the electrodes. A neural response readout system is needed for acquiring the neural activity occurring at the cochlea due to neural stimulation. This data is used by researchers to improve the aforementioned issues. Although all major CI manufacturers have included the possibility of recording neural responses, the possibilities are severely restricted due to the occurrence of saturation in the single channel amplifier and ADC, and the relative high noise levels. This is most clearly illustrated by the fact that objective neural thresholds are mostly found at the upper end of the subjective electrical dynamic range (Hughes, Brown, Lopez and Abbas, 1999). Recording on these relative high levels has as major drawback that different neural waveforms originating from different fibre populations are combined (Briaire and Frijns, 2005). This is most probably also the reason why there is still very limited direct clinical usage for the recorded neural response, irrespective of the very large amount of research effort on the subject. Potentially the neural response data, thresholds, but also the spread of excitation and neural recovery functions, could provide insight in what the optimal stimulation strategy should be, and how to program the current levels of the implant for the individual patients. Especially in very young children this should prove beneficial and lead to increased performance. Researchers are now confronted with the limitations of existing neural response readout systems needed for reading out the evoked compound action potential for their research. These limitations urge the need for a new neural response readout system having a dynamic range of 126dB, that is small, power efficient, has noise levels under 10μV and can handle input signals exceeding the supply voltage. The readout system will be able to read out 256 electrodes simultaneously and is implemented in a MEMS cochlear implant. Existing techniques do not offer solutions to meet the above specifications. An overall readout system design is proposed based on compensation containing an input system, multiplexer, compensation circuit, amplifier and an analog to digital converter (ADC). Existing circuitry does not offer solutions to handle input signals above supply voltage being compact, power efficient, have high dynamic range and have a low noise contribution. Research is performed on developing a new circuit technique based on additive instantaneous companding in order to record the evoked compound action potentials from the stimulated auditory nerve.

DISTAL MARKERS OF PROXIMAL NEOPLASIA: A META-ANALYSIS

Dimitra Dodou, Joost de Winter

Abstract: ABSTRACT The effectiveness of flexible sigmoidoscopy accompanied by colonoscopy relies on the hypothesis that distal findings are markers of proximal lesions. Although three meta-analyses already exist [1 3], there is no consensus about what types of distal findings should lead to full colonoscopy. We conducted a meta-analysis of observational studies to investigate the prevalence of proximal neoplasia (PN) and proximal advanced neoplasia (PAN) in subjects with distal lesions compared to subjects with normal distal colon as a function of the size and histology of the distal findings. A comprehensive literature search was carried out by combining each of the terms "proximal neoplasia", "advanced proximal neoplasia" and "proximal advanced neoplasia" with each of the terms "distal", "hyperplastic", "adenoma", "nonadvanced", "advanced", "sigmoidoscopy", and "colonoscopy" to retrieve observational studies investigating the prevalence of PN and PAN in subjects with distal lesions. Odds ratios (OR) were calculated as the ratio of the number of subjects with proximal lesions in the group of subjects with distal hyperplastic polyps (HP), nonadvanced adenomas (NAA), or advanced neoplasia (AN) to the number of subjects with proximal lesions in the group of subjects with a normal distal colon or a distal colon with no neoplasia. The proportions of PN and PAN that did not have distal markers (so-called isolated proximal neoplasia) were calculated as well. Thirty one studies were identified. HP were a significant predictor of PN (OR=1.7, 95% CI=1.2–2.4), but not of PAN (OR=1.2, 95% CI=0.7–1.8). NAA and AN were predictors of both PN (OR=2.4, 95% CI=2.0–3.1 and OR=3.4, 95% CI=2.4–4.9) and PAN (OR=2.1, 95% CI=1.6–2.8 and OR=5.4, 95% CI=3.3–8.7). Moreover, 60.9% (SD=19.0) of PN and 59.8% (SD=12.6) of PAN were isolated. In conclusion, our meta-analysis showed that not only advanced but also nonadvanced distal lesions are markers of proximal lesions. The existence of isolated PN and PAN signalised that, when considering the value of colonoscopy as a follow-up of flexible sigmoidoscopy, it is important to consider not only the percentage of false positive proximal pathology (i.e., the number of subjects with distal but no proximal lesions), but also the percentage of false negative results, that is, the number of proximal lesions that could not be predicted based on the condition of the distal colon only. These findings have clinical consequences for the development of screening programs for colorectal cancer. REFERENCES [1] S. Dave, S. Hui, K. Kroenke, and T.F. Imperiale, "Is the distal hyperplastic polyp a

marker of proximal neoplasia? A systematic review", JGIM, Vol. 18, pp. 128 137, (2003). [2] J.D. Lewis, K. Ng, K.E. Hung, W.B. Bilker, J.A. Berlin, C. Bresinger, and A.K. Rustgi, "Detection of proximal adenomatous polyps with screening sigmoidoscopy. A systematic review and meta-analysis of screening colonoscopy", Arch. Intern. Med., Vol. 163, pp. 413 420, (2003). [3] O.S. Lin, L.B. Gerson, M.-S. Soon, D.B. Schembre, and R.A. Kozarek, "Risk of proximal colon neoplasia with distal hyperplastic polyps. A meta-analysis", Arch. Intern. Med., Vol. 165, pp. 382 390, (2005).

A FAST AND ROBUST IMPLEMENTATION OF A BONE-REMODELING ALGORITHM

Gianni Campoli, Harrie Weinans, Amir Zadpoor

Abstract: According to the Wolff's tissue adaptation law, the density and morphology of bone is partly controlled by mechanical force, in the dynamic process of bone remodeling. It is not yet well understood how these loading signals are translated into the activity of the cells that resorb old bone (osteoclasts) and generate new bone (osteoblasts). Nevertheless, modeling of the bone tissue adaptation is important not only for improving our understanding of how bone changes over time but also for applying the model in orthopaedics. A well-known model of bone remodeling [1] is implemented in a 3D Finite Element Method (FEM) package. The algorithm aims to obtain a constant value for the strain energy density at every element per unit bone mass by adapting the density and, thus, the mechanical properties of the element. The model includes the presumed sensory role of osteocytes [2], so as they can be considered as a network of sensors that are sensitive to the locally-sensed strains and regulate the tissue adaptation mechanism. The effect of each sensor on its surrounding area is assumed to exponentially decay with the distance from the sensor and be dependent on a diffusing factor, D, which determines the size of the domain of the influence of the sensor. The objective of this work is to present a fast and reliable implementation of this well-known tissue adaptation model such that several criteria are met. First, the model should be mesh-independent. Second, it should be fast and robust so that it is suitable for practical applications. In order to meet these criteria, a version of the tissue adaptation model presented in reference [2] is implemented as a user subroutine in the commercial FEM package ABAQUS. The formulation of the model is slightly modified and a few additional parameters are introduced in the model. The effects of these parameters on the accuracy and computational cost of the model are investigated. The effects of the number and distribution of the sensors on the final converged shape of the tissue are also studied. The results of the model are validated against the previous implementations of the remodeling algorithm. Moreover, it is shown that this implementation of the remodeling algorithm meets the above-mentioned design criteria. REFERENCES [1]H. Weinans, R. Huiskes and H. Grootenboer, "The behavior of adaptive bone-remodeling simulation models", Journal of Biomechanics, Vol. 25, No. 12, pp. 1425 1441, (1992). [2]M. G. Muellender, R. Huiskes, H. Weinans, "A physiological approach to the simulation of bone remodeling as a self-organizational control process", Journal of Biomechanics, Vol. 27, No. 11, pp. 1389 1394, (1994).

CARDIAC LEFT ATRIUM WALL SEGMENTATION FOR CATHETER ABLATION OF ATRIAL FIBRILLATION

Fitsum Mesadi, Peter Rongen, Bart ter Haar Romeny, Hans van Assen

Abstract: Atrial Fibrillation (AF) is a condition related to abnormal electrical activity in the atrium. In recent years, radio-frequency catheter ablation has emerged as an effective treatment option. Knowledge of the left atrium local wall thickness is essential to determine the proper ablation energy and duration. Even though the segmentation of the left atrium (LA) endocardial wall has been investigated relatively well (see e.g. [1]), to our knowledge, accurate and automatic 3D segmentation of the epicardial wall has not yet been presented in literature. The very low contrast edges at the outer surface and the thin LA wall thickness (1.7-4.3mm [2]) make segmentation of the epicardial wall very challenging. In this paper we present an approach that robustly segments these two surfaces after a single seed point selection by the user. The technique is based on rough segmentation of the epi- and endocardial walls, followed by application of an optimization algorithm to accurately find these surfaces. The initial segmentation is based on the Otsu threshold and level set methods [2]. A new knowledge and context-based gradient feature is developed for the analysis of low contrast edges. This knowledge-based gradient is combined with other geometric information to guide the accurate positioning of the epicardial surface. Validation of any low contrast segmentation algorithm is far from trivial due to unreliability of manually segmented ground truth data. A new approach, based on combination of CT and ultrasound images, is being investigated to validate the proposed segmentation algorithm. The left atrium wall segmentation algorithm presented here can easily be extended to other medical image processing problems (which have similar properties). The colon, the left ventricle, the airways, and the gallbladder are some of the areas with thin walls and low contrast at the outer surface and hence can easily benefit from the proposed algorithm.

FEATURE BASED CARDIAC MOTION ESTIMATION USING COVARIANT DERIVATIVES AND HELMHOLTZ DECOMPOSITION

Alessandro Becciu, Remco Duits, Luc Florack, Bart Janssen, Bart ter Haar Romeny, Hans van Assen

Abstract: The investigation and quantification of cardiac movement is important for the assessment of cardiac abnormalities and treatment effectiveness. Typically, the motion of the endo- and epicardial wall is assessed. However, a method is needed to establish the motion and deformation parameters within the myocard, preferably at voxel resolution. Therefore we consider a new aperture-problem-free method to track cardiac motion from 2-dimensional MR tagged image sequences and corresponding sine-phase images. Tracking is achieved by following the movement of stable anchor points, i.e. scale-space maxima, yielding a sparse sampling of the unknown dense optic flow vector field. Interpolation/reconstruction of the velocity field is then carried out by minimizing an energy functional expressed in covariant derivatives (rather than standard derivatives). These covariant derivatives are used to express prior knowledge about the velocity field in the variational framework employed. They turn out to be highly effective. Furthermore, the optic flow vector field is decomposed in a divergence-free and a rotation-free part, using a newly developed multi-scale Helmholtz decomposition algorithm. Finally, this multi-scale Helmholtz decomposition is combined with the vector field reconstruction based on covariant derivatives in a single algorithm. We present experiments of cardiac motion estimation for ground-truth phantom data, and a selected set of patients with known infarcted regions. The experiments show that both the inclusion of covariant derivatives and of the multi-scale Helmholtz decomposition markedly improves the accuracy of the optic flow reconstruction. REFERENCES [1] A. Becciu, H.C. van Assen, L.M.J. Florack, S. Kozerke, V.J. Roode, B.M. ter Haar Romenij, "A multiscale feature based optic flow method for 3D cardiac motion estimation", Lecture Notes in Computer Science, 5567, 588-599, (2009). [2] A. Becciu, B.J. Janssen, H.C. van Assen, L.M.J. Florack, V.J. Roode, B.M. ter Haar Romenij, "Extraction of cardiac motion using scale-space features points and gauged reconstruction", Lecture Notes in Computer Science, 5702, 598-605, (2009).

BME EDUCATION – COLLABORATION WITH CHINA

Bart ter Haar Romeny, Yan Kang, Han van Triest, Peter Hilbers

Abstract: The TU/e is focusing on internationalization. At the same time, Philips Healthcare is expanding its market to China, and has set up since 2005 a joint venture with Neusoft Medical Systems, the largest medical imaging company in China, located in Shenyang (NE China, capital of Liaoning Province, the 6th largest city in China) and now having over 16.000 employees. To create new engineers, a new Biomedical Engineering Department was established at Northeastern University in 2005: the Sino-Dutch Biomedical and Information Engineering School of Northeastern University (BMIE). With a target of 1000 students in 2015, the school now counts 470 students, with a BSc, MSc and PhD program. The main focus areas are medical imaging, bio-informatics, and medical instrumentation. The educational system of TU/e has been adopted as the leading way of teaching, based on its successful use of 'design centered learning' (DCL), and the balance between engineering and biological knowlegde and skills. TU/e, BMIE, Philips and Neusoft signed a 20-year collaboration contract to get the school to a mature level. The best BMIE students get the opportunity to do the MSc track at BME-TU/e, by a dedicated grant of the partners. Prof. Kang, dean of BMIE, also heads the Neusoft Medical Imaging research, linking the industrial and educational values and targets. Teachers of TU/e regularly teach at BMIE. DCL emphasizes the articulation of brainstorming skills, analysis and design of complex processes, develop, implement and evaluate projects, and it promotes the creativity, leading to more proactive students. Especially in China this new method is a revolution, compared to the traditional oral-course based system. Students are enthousiast, and the need for an expanding teacher base is recognized. English is improving rapidly, especially the younger generation is fluent. The DCL environment is enhanced with a rich set of BME equipment (PACS, EEG/MEG, ultrasound, X-ray, cone-beam CT, 3D visualization software etc.). The high-level design software environment Mathematica successfully invites the students to manipulate parameters, 'play with math', and interactively visualize results of any complexity quickly. Oral lectures are de-emphesized, solving a complex problem with a team gets more time. The current TU/e time allocated to DCL is 50% in the BSc phase. Roles for good team management by the students are based on the roles developed by Belbin and coworkers at Cambridge University. Students intermittendly take leadership roles, and grade themselves in a peer-review process. REFERENCES [1] M.J. Hannafin, S.M. Land, "The foundations and assumptions of technology-enhanced student-centered learning environments", Instructional Science 25: 167-202, Kluwer Academic Publishers, 1997 . [2] Biomedical Engineering Education at TU/e: Skill for Design Centered Learning, https://ai5.wtb.tue.nl/doccontent/vaardighedenBMT/default.php.

A WINDKESSEL MODEL DESCRIPTION OF CEREBRAL AUTOREGULATION IN ALZHEIMER'S DISEASE: increased vascular resistance and lowered compliance.

Erik Gommer, Esther Martens, Pauline Aalten, Frans Verhey, Inez Ramakers, Werner Mess, Jos Reulen

Abstract: There is increasing evidence that cerebrovascular dysfunction plays a role not only in vascular causes of cognitive impairment but also in Alzheimer's disease (AD) [1]. In our study dynamic cerebral autoregulation (dCA) was investigated in AD patients and in patients diagnosed as mild cognitive impairment (MCI), possibly a prodromal state of AD. dCA was quantified by computation of the linear transfer function between arterial blood pressure (ABP) as input and cerebral blood flow velocity (CBFV) as output resulting in transfer function gain and phase. Results were also evaluated using a 3-parameter Windkessel model (WM) as described by Zhang et al [2]. We hypothesize that dCA is impaired in AD compared to matched controls (C) and that in MCI dCA is "in between" AD and C. We included 17 AD, 19 MCI patients and 20 C. The groups were matched for age, gender and level of education. The electrocardiogram (ECG) and non-invasive finger ABP were measured using a Task Force Monitor (CN Systems, Austria). A

transcranial Doppler system (Multidop X4, DWL, Sipplingen, Germany) was used to measure CBFV in the main stem of both the right and left middle cerebral artery. Two 2 MHz probes were held in position by a special frame. Patients were in supine position with their eyes open during all recordings. Phase and gain were evaluated for different frequency bands of autoregulation namely Total (0.04-0.11 Hz) , VLF (0.04-0.06 Hz), 01 (0.1 Hz) , LF (0.06-0.11 Hz). Also the cerebrovascular resistance index CVRi (i.e. mean ABP/ mean CBFV) was computed. GainTotal (mean±se) was significantly lower in AD (1.07±0.09) compared to C (1.37±0.08, p=0.04). CVRi was significantly higher in AD compared to C (2.8±0.15 vs. 2.1±0.14, p=0.004). In terms of the WM approach, in the order C->MCI->AD subjects show equal arterial resistance, an increase in peripheral vasculature resistance and a decrease in vasculature compliance. Results of TFA will be discussed in relation to the WM approach. Possibly characterization of dCA by Windkessel model parameters provides a new way for individual patient classification. REFERENCES [1] C. Iadecola, "The overlap between neurodegenerative and vascular factors in the pathogenesis of dementia", Acta Neuropathol, Vol. 120, pp. 287-296, (2010) [2] R. Zhang, K. Behbehani, B.D. Levine, "Dynamic pressure-flow relationship of the cerebral circulation during acute increase in arterial pressure", J Physiol, Vol. 587, pp. 2567-2577, (2009).

DEVELOPMENT OF MRI COMPATIBLE AND STEERABLE INSTRUMENT FOR MINIMAL INVASIVE INTERVENTIONS

Helene Clogenson, Chunman Fan, Paul Breedveld, John van den Dobbelsteen, Jenny Dankelman

Abstract: Endovascular interventions are performed under fluoroscopy/angiography guidance that exposes patient and staff to accumulating doses of ionizing radiation and is limited to 2-dimensional images. Magnetic Resonance Imaging (MRI) provides superior soft-tissue contrast, offers 3D reconstruction capabilities and allows the depiction of functional parameters such as blood flow, tissue oxygenation or diffusion. MRI does not expose patients and staff to ionizing radiation and may even allow some endovascular interventions without the use of contrast media. MRI-guided interventions require MR compatible instruments to become part of clinical routine work [1, 2]. Furthermore, manoeuvrability of catheters and guide wires determines whether the target can be successfully reached and hence to a great extent affects the efficiency of the procedure and its success rate. Conventional catheters are difficult to manipulate, steer and control so that there is an accompanying risk of complications, such as dissection or perforation. Steerable instruments offer improved manoeuvrability and may thereby reduce operating time and the risk of complications [3]. The goal of this project is to develop MRI compatible and steerable instrument for minimally invasive intervention. Recently, metallic steerable instruments, inspired on the anatomy of squid tentacles have been developed at TUDelft. Within the current project, a MRI compatible guidewire with one direction of steerability (finger like steerability) will be designed based on this so-called cable-ring mechanism. Ferromagnetic components have to be substituted, due to their non-MRI compatibility. Non-metallic wire will be used to avoid resonance due to the radiofrequency pulses in the MR scanner that otherwise could result in heat production along the metallic wire. Based on the results of this study, a MRI compatible steerable instrument with more degrees of freedom will be developed. This project is part of the European Union initial training network IIIOS (Integrated Interventional Imaging Operating System). REFERENCES 1. Buecker A, Safety of MRI-guided vascular interventions. Minim Invasive Ther Allied Technol., 2006. 15(2): p. 65-70. 2. Kos S, H.R., Hofmann E, Quick HH, Kuehl H, Aker S, Kaiser GM, Borm PJ, Jacob AL, Bilecen D, Feasibility of real-time magnetic resonance-guided angioplasty and stenting of renal arteries in vitro and in Swine, using a new polyetheretherketone-based magnetic resonance-compatible guidewire. Invest Radiol., 2009. 44(4): p. 234-41. 3. Fu Y, L.H., Huang W, Wang S, Liang Z., Steerable catheters in minimally invasive vascular surgery Int J Med Robot., 2009. 5(4): p. 381-91.

CAROTID SEGMENTATION AND CAROTID BIFURCATION ANGLE QUANTIFICATION IN BLACK BLOOD MRA

Hui Tang, Robbert van Onkelen, Theo van Walsum, Reinhard Hameeteman, Michiel Schaap, Fufa Tori, Quirijn van den Bouwhuijsen, Jacqueline Witteman, Aad van der Lugt, Lucas van Vliet, Wiro Niessen

Abstract: Carotid arthrosclerosis, i.e. plaque build-up in the arterial wall, is one of the major causes of stroke. To resolve the mechanisms behind plaque formation, many research institutes are investigating plaque formation, plaque growth and the factors affecting plaque formation and growth [1]. Thomas et al. showed that the inter subject variation in geometry of the carotid bifurcation significantly increases with age and early atherosclerotic disease progression [1]. Whether an individual's geometry will predict the development and progression of atherosclerosis is still unclear and needs to be investigated. In this paper, we proposed a geodesic active contours based segmentation method for accurate and robust quantification of the carotid bifurcation angle in Black Blood MRA data. First, in the pre-processing steps, we use the N3 bias correction method to remove the intensity inhomogeneity and anisotropic edge enhanced diffusion to remove the noise while preserving the centrelines. After pre-processing, we use a 3D geodesic active contour which includes both gradient in intensity features to segment the carotids. The image intensity term is based on an estimate of the local fore- and background intensities, using k-means clustering. The parameters in this method are optimized in 20 representative training datasets, and the optimized method is evaluated on 76 training data sets which are taken from a longitudinal population study[2]. Finally, we quantify the bifurcation angle using publically available software VMTK[3] for both the semi-automatically segmented and the manually annotated lumen to study the accuracy of quantification. The bifurcation angle obtained from the segmented lumen corresponds well with the angle derived from the manual lumen segmentation, which demonstrates that the method has large potential to replace manual segmentations for extracting the carotid bifurcation angle from Black Blood MRA data.

Back